Comparing the elliptic Ruijsenaars–Schneider model to the finite volume sine-Gordon theory

Zoltan Bajnok^{1,2}, Apor Roth^{1,3} November 21, 2025

Wigner Research Centre for Physics
 Konkoly-Thege Miklós u. 29-33, 1121 Budapest , Hungary
 Institute of Theoretical Physics and Mark Kac Center for Complex Systems Research, Jagiellonian University, 30-348 Kraków, Poland
 Roland Eötvös University, Department for Theoretical Physics, 1117 Budapest, Pázmány sétány 1/A, Hungary

Abstract

We compare the spectrum of the elliptic Ruijsenaars—Schneider model with the finite-size spectrum of the sine-Gordon model, highlighting both their similarities and differences. Our analysis focuses on the two-particle sector in the center-of-mass frame. At the free point, we carry out an analytic comparison, while at generic couplings we employ non-perturbative numerical calculations based on the truncated Hilbert space method adapted to difference operators. To benchmark this numerical approach, we first study the trigonometric limit, where analytic results are available. We then examine in detail the non-relativistic limit, which encompasses the rational, trigonometric, hyperbolic, and elliptic Calogero—Moser—Sutherland models. Finally, we compare the Bethe—Yang momentum quantization conditions, derived from infinite-volume scattering phases, with the exact finite-volume solutions. We find that these conditions hold exactly in the rational and trigonometric cases, but acquire finite-size corrections in the hyperbolic and elliptic cases, both for the relativistic model and its non-relativistic limit, however, these corrections are different in quantum field theories and in many body systems

1 Introduction

Integrable quantum field theories (QFTs) are important for several reasons [1, 2, 3]. They provide simplified settings in which strongly coupled, non-perturbative phenomena can be analysed exactly. While QFTs underpin the fundamental interactions of nature, they also describe condensed matter systems and play central roles in statistical physics. In higher dimensions, interacting QFTs are extremely complicated and generally not exactly solvable. In contrast, in two space-time dimensions there exist integrable QFTs that, while still sharing many essential features with realistic systems, remain analytically tractable. These theories are not only valuable as simplified laboratories for quantum phenomena but are also of intrinsic mathematical interest, being deeply connected to representation theory, quantum groups, and other areas of mathematics.

In integrable theories the scattering matrix is purely elastic: there is no particle production, and particles retain their velocities during scattering [4]. This property is already visible at the classical level. In the sine-Gordon model, the finite-energy classical solutions consist of solitons, anti-solitons, and their bound states, the breathers [5]. During time evolution, these excitations preserve their velocities. The interaction manifests only through time delays, which can be obtained by summing the individual delays a particle would experience when scattering off each of the others separately. In this integrable field theory there is no dispersion, and asymptotic solutions consist of well-separated wave fronts that retain their profiles throughout the scattering process. These localised excitations can be interpreted as particles.

Ruijsenaars and Schneider posed the question of whether a relativistically invariant multi-particle system (not a field theory) could reproduce the sine-Gordon time delays. They answered affirmatively by constructing the hyperbolic Ruijsenaars–Schneider (RS) model, which is relativistically invariant and whose time delays coincide exactly with those of the sine-Gordon model [6]. Later, Ruijsenaars extended this correspondence to the quantum level, showing that the sine-Gordon scattering phases can also be reproduced by the quantum RS model [7], see also [8, 9] and references therein. This remarkable result suggests that an integrable quantum field theory can, in certain respects, be equivalent to a quantum mechanical system. In the present work, we address the question of whether this correspondence can be extended from infinite to finite volume. The *elliptic* RS model can be viewed as the finite-volume generalization of the hyperbolic RS model, (for recent reviews see [10, 11]). Our aim is therefore to compare its energy spectrum with that of the finite-volume sine-Gordon theory.

In quantum field theory, finite-size effects are governed by the scattering matrix. If the same holds in quantum mechanical systems, then a correspondence with QFT spectra becomes plausible. In QFT, the leading large-volume corrections are captured by the Bethe–Yang equations [12, 13]. These enforce periodicity of the multiparticle wavefunction by incorporating the scattering phases particles acquire upon crossing one another, thereby leading to momentum quantization. However, additional corrections arise from vacuum polarisation: the vacuum is populated by particle–antiparticle pairs that propagate around the finite spatial volume and annihilate, producing exponentially suppressed contributions [14, 15]. These effects modify the Bethe–Yang equations; they are known as Lüscher corrections [16]. When multi-particle processes are included, the full finite-size spectrum can be obtained through the thermodynamic Bethe ansatz (TBA) [13].

For quantum mechanical systems, no analogous analytic framework is currently available. We therefore rely primarily on numerical comparisons (with analytic checks at specific points of the parameter space). To validate our numerical methods, we examine various limiting cases of the elliptic RS model. These include the non-relativistic Calogero–Moser–Sutherland models [17, 18, 19, 20], as well as the rational, trigonometric, and hyperbolic limits, where exact results exist for general couplings. For the quantum mechanical case, we adapt the non-perturbative truncated Hilbert space method, benchmarking it against exact solutions whenever possible. We then compare the numerical spectrum of the quantum elliptic RS model with the spectrum obtained from the nonlinear integral equation (NLIE) describing the exact finite-volume sine-Gordon theory [21, 22, 23]. Our analysis, restricted to the two-soliton sector, demonstrates that the two models differ at finite volume.

The paper is organized as follows: In Section 2 we introduce the sine-Gordon model and describe its finite-size energy spectrum. Section 3 presents the elliptic RS model, together with its various limits (Calogero–Moser, rational, trigonometric, and hyperbolic), and recalls the correspondence between the hyperbolic RS model and the sine-Gordon theory. In Section 4 we introduce the truncated Hilbert space method and apply it to study the finite-size spectra of the trigonometric and elliptic CMS systems, analyzing their relation to the Bethe–Yang equations. Section 5 generalizes the method to the relativistic RS cases and Section 6 compares their spectra with those of the finite-volume sine-Gordon model. Finally, the paper ends with concluding remarks.

2 Sine-Gordon model

The sine-Gordon model is an integrable 1+1 dimensional field theory of a real scalar field with the Lagrangian [5]

$$\mathcal{L} = \frac{1}{2} \partial_{\mu} \varphi \partial^{\mu} \varphi - \frac{m^2}{\beta^2} (1 - \cos \beta \varphi)$$
 (2.1)

2.1 Classical theory

The classical theory admits static, finite energy, localised solutions

$$\varphi_{\pm}(x) = \pm \frac{4}{\beta} \arctan\left(e^{m(x-x_0)}\right)$$
(2.2)

which interpolate between neighbouring minima of the potential. Their energy density is localised around x_0 and they are called the soliton and the anti-soliton. Since the theory is relativistically invariant, the boost transformation $(x,t) \to (x \cosh \theta + t \sinh \theta, t \cosh \theta + x \sinh \theta)$ leaves the Lagrangian

invariant. As a consequence the boosted solutions $\varphi_{\pm}(x\cosh\theta+t\sinh\theta)$ keep their shape forever and travel with velocity $v=\tanh\theta$. These solitary wave solutions of the field theory are called for short solitons. They have localised energy densities and can be interpreted as particles. The existence of infinitely many conserved charges implies that one can construct scattering solutions, which preserve the number of particles and their velocities. In particular, the soliton-soliton scattering solution takes the form

$$\varphi_{++}(x,t) = \frac{4}{\beta} \arctan\left(\frac{e^{x \cosh \theta + t \sinh \theta - x_1} + e^{x \cosh \theta - t \sinh \theta - x_2}}{1 - e^{2x \cosh \theta - x_1 - x_2 + 2 \ln \tanh \theta}}\right)$$
(2.3)

Asymptotically for $t \to \mp \infty$, they describe two solitons in the center of mass frame moving oppositely with velocities $v = \pm \tanh \theta$. The difference compared to the free motion is the time delay or space displacement $\Delta x = 2 \ln \tanh \theta$ they experienced

$$\lim_{t \to +\infty} \varphi_{++}(x,t) = \varphi_{+}((x \pm \Delta x/2)\cosh\theta + t\sinh\theta) + \varphi_{+}((x \pm \Delta x/2)\cosh\theta - t\sinh\theta)$$
 (2.4)

The information on the interaction can be encoded into the energy dependence of this space displacement. Integrability implies that space displacements of multi-particle states add up and depend only on the individual two particle interactions. This is a consequence of the fact that the space displacement depends purely on the rapidity difference of the particles and not on their actual initial positions x_i .

Ruijsenaars and Schneider parametrized the sine-Gordon soliton-soliton solution as

$$\varphi_{++}(x,t) = \frac{4}{\beta}\arctan\left(e^{u_1(x,t)}\right) + \frac{4}{\beta}\arctan\left(e^{u_2(x,t)}\right)$$
(2.5)

and asked the question, what is the effective dynamics of the $u_i(x,t)$ "particle" trajectories. This is how they constructed the hyperbolic RS models [6]. This theory is a relativistically invariant multiparticle theory, which reproduces also the multi-particle time delays of the sine-Gordon theory. Evenmore, its proper quantization reproduced the exact scattering phases of the quantum sine-Gordon theory. See section 3 for details.

2.2 Quantum theory

The quantum sine-Gordon theory is an integrable quantum field theory. Being such, it is characterized by its particle content and their scattering matrix [4]. The quantum theory always contains the soliton and the anti-soliton, while the rest of the spectrum depends on the coupling constant, which is parametrized as

$$p = \frac{\beta^2}{8\pi - \beta^2} \tag{2.6}$$

For p>1 the soliton and the anti-soliton repulse each other and there are no more particles in the spectrum. For p=1 these particles do not interact and we have a free model. For 0< p<1 the interaction is attractive: solitons and anti-solitons form neutral boundstates with masses $m_n=2M\sin\frac{\pi pn}{2}$, where M is the soliton mass and $n\leq [1/p]$. The soliton and anti-soliton compose into a mass degenerate doublet, which scatters on itself by a four by four matrix, which is the function of the rapidity difference. Unitarity, crossing symmetry and the Yang-Baxter equation fixes the soliton-soliton scattering to be

$$S_{++}^{++}(\theta) = S_{--}^{--}(\theta) \equiv S(\theta) = -e^{i\chi(\theta)} \quad ; \quad \chi(\theta) = \int_0^\infty dk \frac{\sin k\theta}{k} \frac{\sinh \frac{\pi(p-1)k}{2}}{\sinh \frac{\pi pk}{2} \cosh \frac{\pi k}{2}}$$
(2.7)

while the other non-zero scatterings are

$$S_{+-}^{+-}(\theta) = S_{-+}^{-+}(\theta) = S(\theta) \frac{\sinh \frac{\theta}{p}}{\sinh \frac{i\pi - \theta}{p}} \quad ; \quad S_{+-}^{-+}(\theta) = S_{-+}^{+-}(\theta) = S(\theta) \frac{\sinh \frac{i\pi}{p}}{\sinh \frac{i\pi - \theta}{p}}$$
(2.8)

The very same scattering coefficients was reproduced by the hyperbolic quantum Ruijsenaars-Schneider model [7]. This established the connection between the two models in infinite volume. Our aim is to see, how this correspondence could be extended at finite volume with periodic boundary condition.

2.3 Quantum theory with perodic boundary condition

In relativistic quantum field theories the full finite size spectrum can be described based on the scattering matrix. One distinguished feature, different from quantum mechanical systems, is the finite size correction of the vacuum. This is due to the fact that the vacuum is the sea of virtual particle anti-particle pairs, whos interaction can be taken into account in the sine-Gordon theory via the Destri - de Vega equation [21]

$$E_0(L) = -M \int \frac{dx}{2\pi i} \sinh(x + i\eta) \log(1 + e^{iZ(x+i\eta)})$$
$$+ M \int \frac{dx}{2\pi i} \sinh(x - i\eta) \log(1 + e^{-iZ(x-i\eta)})$$
(2.9)

where the counting function Z(x) satisfies

$$Z(x) = ML \sinh x + \int_{-\infty}^{\infty} \frac{dy}{2\pi i} G(x - y - i\eta) \log(1 + e^{iZ(y + i\eta)})$$
$$- \int_{-\infty}^{\infty} \frac{dy}{2\pi i} G(x - y + i\eta) \log(1 + e^{-iZ(y - i\eta)})$$
(2.10)

and η is an arbitrary small positive parameter while M is the soliton mass. The kernel is the derivative of the scattering matrix phase

$$G(x) = \partial_x \chi(x) = \int_{-\infty}^{\infty} dk \, e^{ikx} \frac{\sinh \frac{\pi(p-1)k}{2}}{2 \sinh \frac{\pi pk}{2} \cosh \frac{\pi k}{2}}$$
(2.11)

Once we put two solitons with opposite rapidities θ and $-\theta$ into the vacuum the energy is modified as [23]

$$E(L) = 2M \cosh \theta - M \int \frac{dx}{2\pi i} \sinh(x + i\eta) \log(1 + e^{iZ(x+i\eta)})$$
$$+ M \int \frac{dx}{2\pi i} \sinh(x - i\eta) \log(1 + e^{-iZ(x-i\eta)})$$
(2.12)

where the counting function Z(x) now describes how the solitons polarise the interacting vacuum

$$Z(x) = ML \sinh x + \chi(x - \theta) + \int_{-\infty}^{\infty} \frac{dy}{2\pi i} G(x - y - i\eta) \log(1 + e^{iZ(y + i\eta)}) + \chi(x + \theta) - \int_{-\infty}^{\infty} \frac{dy}{2\pi i} G(x - y + i\eta) \log(1 + e^{-iZ(y - i\eta)})$$
(2.13)

the rapidity is determined by the quantisation condition as $Z(\theta) = 2\pi(n + \frac{1}{2})$ and $\chi(0) = 0$.

These equations can be solved exactly only for p = 1 when G(x) = 0. In general, one can make a large volume expansion. For very large volumes the integral terms can be neglected and the quantisation condition

$$Z(\theta) = ML \sinh \theta + \chi(2\theta) + \dots = 2\pi n + \pi \tag{2.14}$$

is the logarithm of the Bethe–Yang equation, which, for two particles with opposite rapidities, takes the form

$$e^{iML\sinh\theta}S_{++}^{++}(2\theta) = 1$$
 (2.15)

Its solution provides the quantised rapidities θ_n , which gives the energy as $E(L) = 2M \cosh \theta_n + O(e^{-ML})$.

One can expand the integral equations systematically to calculate the exponentially small e^{-ML} corrections. The leading term is the so called Lüscher correction [14, 15]. Lüscher calculated this correction for a single standing particle, which was then extended to moving particles in [24, 25] and for multiparticle states in [16]. The generic form of the second order correction is given in [26].

In general, the equations cannot be solved analytically, however, they can be solved very precisely numerically. In so doing, we discretise the functions on a grid and perform the convolution by Fourier transform, where the explicit Fourier transform of the kernel can be used.

Technically, we evaluate $iZ(x+i\eta)$

$$iZ(x+i\eta) = iML \sinh(x+i\eta) + i\chi(x+i\eta-\theta) + \int_{-\infty}^{\infty} \frac{dx}{2\pi} G(x-y) \log(1+e^{iZ(y+i\eta)}) + i\chi(x+i\eta+\theta) - \int_{-\infty}^{\infty} \frac{dx}{2\pi} G(x-y+i2\eta) \log(1+e^{-iZ^*(y+i\eta)})$$
(2.16)

where we used that $Z(x-i\eta)=Z^*(x+i\eta)$ and obtained a closed system for $iZ(x+i\eta)$ for a given θ . In evaluating $\chi(\theta)$ and $\chi(x+i\eta)$ we use

$$i\chi(\theta) = \int_0^\infty dk \frac{e^{ik\theta} - e^{-ik\theta}}{k} \frac{\sinh\frac{\pi(p-1)k}{2}}{2\sinh\frac{\pi pk}{2}\cosh\frac{\pi k}{2}}$$
(2.17)

and

$$i\chi(x+i\eta) = \int_{-\infty}^{\infty} \frac{dk}{k} e^{ikx} \frac{e^{-k\eta} \sinh\frac{\pi(p-1)k}{2}}{2\sinh\frac{\pi pk}{2}\cosh\frac{\pi k}{2}}$$
 (2.18)

At the quantisation condition we take

$$Z(\theta) = ML \sinh(\theta) + \int_{-\infty}^{\infty} \frac{dx}{2\pi i} G(\theta - y - i\eta) \log(1 + e^{iZ(y + i\eta)})$$
$$+ \chi(2\theta) - \int_{-\infty}^{\infty} \frac{dx}{2\pi i} G(\theta - y + i\eta) \log(1 + e^{-iZ^*(y + i\eta)})$$
(2.19)

We can solve these equation by iteration with arbitrary precision. We start from the Bethe–Yang values and update $iZ(x+i\eta)$ and θ in each step until we reach the prescribed precision. We would like to compare the obtained finite volume spectrum to the elliptic Ruijsenaars-Schneider model, so we recall their definition now.

3 Ruijsenaars-Schneider models

The RS multiparticle models are very unique of being relativistically invariant with potential interaction of the same type. Their Hamiltonian and momentum takes the following form [6, 27]

$$H = m \sum_{j=1}^{N} \cosh \theta_{j} \prod_{1 \le j \le k \le N} f(q_{j} - q_{k}) \quad ; \quad P = m \sum_{j=1}^{N} \sinh \theta_{j} \prod_{1 \le j \le k \le N} f(q_{j} - q_{k})$$
 (3.1)

where θ_j and q_i are canonically conjugated phase space coordinates: $\{\theta_j, q_i\} = \delta_{ij}$ and we put the speed of light to 1. Together with the boost operator $B = -\sum_{i=1}^{N} q_i$ they generate the 1+1 dimensional Poincare algebra

$$\{H, P\} = 0 \quad ; \quad \{H, B\} = P \quad ; \quad \{P, B\} = H$$
 (3.2)

The first commutator restricts the potential to the form

$$f(q)^2 = a + b\wp(q, L, \frac{i\pi}{d}) \tag{3.3}$$

where \wp is the Weierstrass \wp -function with real periodicity L, and imaginary periodicity π/d , while a,b are real parameters. This model is referred to as the elliptic RS model. In the free case, f=1, the form of the energy and momentum indicates that θ should be interpreted as the rapidity and q, being its conjugate, cannot be the space coordinate. The canonically conjugated momentum and space coordinates are as $p_i = m \sinh \theta_i$ and $x_i = \frac{q_i}{m \cosh \theta_i}$ [6]. Thus the coordinate x_i seems like the Lorentz contracted q_i , implying that the q_i phase space coordinate should be understood as the coordinate in the particle's own rest frame. In this sense the interaction is rather peculiar depending on the coordinate difference of the particles' rest coordinates, but this is the form, which ensures the relativistic invariance. The theory is actually invariant under a higher symmetry. The quantities

$$S_{\pm l} = \sum_{\substack{I \subset \{1, \dots, N\}\\|I| = l}} \exp\left(\pm \sum_{j \in I} \theta_j\right) \prod_{\substack{j \in I\\k \notin I}} f(q_j - q_k),$$
(3.4)

all Poisson commute, including the Hamiltonian and momentum, which can be expressed as $\frac{m}{2}(S_1 \pm S_{-1})$, respectively [6]. This implies that the model is integrable in the Liouville sense: we have as many conserved charges as many particles.

Various limits are interesting. The hyperbolic limit is when the real period goes to infinity $L \to \infty$:

$$\wp(q, \infty, \frac{i\pi}{d}) = \frac{d^2}{3} + \frac{d^2}{\sinh^2(dq)} \quad ; \quad f^2(q) = 1 + \frac{\sin^2(d\lambda)}{\sinh^2(dq)}$$
 (3.5)

leading to particles on the whole line. Here we choose specific a,b coefficients. This model is related to the classical sine-Gordon theory [6]. Let us choose some initial coordinates on the phase space $u = \{(\theta_i, q_i)\}$ and generate a flow with the time (H) and space (P) evolution generators as $u_i(x,t) = (e^{tH-xP}u)|_{q_i} \equiv q_i(x,t)$. It can be shown that for d=1/2 and $\lambda=\pi$

$$\varphi(x,t) = \frac{4}{\beta} \sum_{i=1}^{N} \arctan(e^{u_j(x,t)})$$
(3.6)

satisfies the sine-Gordon equation of motion. In the two particle case this leads to the soliton-soliton solution. Observe that the relation between the particles' physical trajectories and u_i is rather involved [28].

In the trigonometric limit the imaginary period goes to infinity $d \to 0$, which formulates the interactions on the circle

$$\wp(q, L, i\infty) = -\frac{\pi^2}{3L^2} + \frac{\pi^2}{L^2 \sin^2(\frac{\pi}{L}q)} \quad ; \quad f^2(q) = 1 + \frac{\sinh^2(\pi\lambda/L)}{\sin^2(\pi q/L)}$$
(3.7)

If we send both periods to infinity we obtain the rational model

$$\wp(x, \infty, i\infty) = \frac{1}{q^2} \quad ; \quad f^2(q) = 1 + \frac{\lambda^2}{q^2}$$
 (3.8)

Let us see now, how we could quantise these non-standard systems.

3.1 Quantum models

Following Ruijsenaars, we quantise the canonical variables as $(\theta_j, q_j) \to (-i\partial_{q_j}, q_j)$. We set $\hbar = 1$ and m = 1. In the free case f = 1, the Hamiltonian takes the form [27]

$$H = \frac{1}{2} \sum_{j=1}^{N} (e^{-i\partial_{q_j}} + e^{i\partial_{q_j}}) \equiv \frac{1}{2} \sum_{j=1}^{N} (T_j^{+1} + T_j^{-1})$$
(3.9)

where the shift operators act as

$$T_j^{\pm 1} f(q_1, \dots, q_j, \dots, q_N) = f(q_1, \dots, q_j \mp i, \dots, q_N)$$
 (3.10)

The eigenfunctions take the form [27]

$$H\psi(\{q\}) = E\psi(\{q\}) \quad ; \quad \psi(\{q\}) = e^{i\sum_{j=1}^{N} \theta_j q_j}$$
 (3.11)

with the energy and momentum eigenvalues

$$E = \sum_{i=1}^{N} \cosh \theta_j \quad ; \quad P = \sum_{i=1}^{N} \cosh \theta_j \tag{3.12}$$

Thus the θ_j s are the correctly normalised rapidity variables. The wave function is a bit strange as it contains the q_j variables in the exponents instead of the coordinates x_j .

In defining the quantum versions of the interacting Hamiltonians we have to face with ordering problems between $T_j^{\pm 1}$ and the potential terms $f(q_i - q_j)$. Ruijsenaars solved this problem by introducing the factorisation of the potential into $f(q) = f_+(q)f_-(q)$ and demanding that the appropriately ordered quantum conserved quantities

$$S_{\pm l} = \sum_{\substack{I \subset \{1, \dots, N\} \\ |I| = l}} \prod_{\substack{j \in I \\ k \notin I}} f_{\mp}(q_j - q_k) T_j^{\pm 1} \prod_{\substack{j \in I \\ k \notin I}} f_{\pm}(q_j - q_k).$$
 (3.13)

commute. He found the following expressions [29, 27]:

$$f_{\pm}(q) = \begin{cases} \left(1 \pm i\frac{\lambda}{q}\right)^{1/2} & \text{rational} \\ \left(\frac{\sinh(d(q\pm i\lambda))}{\sinh(dq)}\right)^{1/2} & \text{hyperbolic} \\ \left(\frac{\sin(\pi(q\pm i\lambda)/L)}{\sin(\pi q/L)}\right)^{1/2} & \text{trigonometric} \\ \left(\frac{\sigma(q\pm i\lambda,L,i\pi/d)}{\sigma(q,L,i\pi/d)}\right)^{1/2} & \text{elliptic} \end{cases}$$

$$(3.14)$$

where $\sigma(q, \pi/L, id)$ is the quasi-periodic Weierstrass sigma-function. It is related to the Weierstrass \wp -function by the following functional relation [30]:

$$\wp(z) - \wp(u) = -\frac{\sigma(z+u)\sigma(z-u)}{\sigma^2(z)\sigma^2(u)}, \qquad (3.15)$$

which guarantees $f(q) = f_{+}(q)f_{-}(q)$. The rational, hyperbolic and trigonometric systems (3.14), can be obtained from the elliptic one as [27]:

$$\sigma(q, \infty, i\pi/d) = \frac{\sinh dq}{d} \exp\left(-\frac{d^2}{6}q^2\right)$$
(3.16)

$$\sigma(q, L, i\infty) = \frac{\sin \pi q/L}{\pi/L} \exp\left(-\frac{\pi^2}{6L^2}q^2\right)$$
(3.17)

$$\sigma(q, \infty, i\infty) = q. \tag{3.18}$$

It is instructive to investigate the non-relativistic limit of these models, the Calogero-Sutherland-Moser systems [18, 19]. To obtain these systems one can restore the dependence on the speed of light $q \to mcq$, $\theta \to \theta/mc$, $d \to dmc$, $L \to L/mc$ and take the $c \to \infty$ limit. The result is a usual quantum many body system, which in the physical coordinates reads as

$$\mathcal{H} = -\frac{1}{2m} \sum_{i=1}^{N} \partial_{x_i}^2 + \frac{\lambda(\lambda - 1)}{2m} \sum_{1 \le j \le k \le N} V(x_i - x_j)$$
(3.19)

with the potentials [31]

$$V = \begin{cases} V_{\text{rat}} = 1/x^2 & \text{rational} \\ V_{\text{hyp}} = d^2/\sinh^2(dx) & \text{hyperbolic} \\ V_{\text{trig}} = \pi^2/\left(L^2\sin^2(\pi x/L)\right) & \text{trigonometric} \\ V_{\text{ell}} = \wp(x, L, i\pi/d) & \text{elliptic} \end{cases}$$
(3.20)

In the following we recall the solutions of these systems and the relations between them, together with an efficient numerical approach to calculate their finite size spectra.

4 Calogero-Moser-Sutherland systems and the truncated Hilbert space method

In this section we investigate the CMS models for two-particles in the center of mass frame at generic couplings. The appropriately scaled Hamiltonian leads to the Schrödinger equation

$$\mathcal{H}\psi \equiv (-\partial_x^2 + \lambda(\lambda - 1)V(x))\psi = E\psi \tag{4.1}$$

and describes the motion of a single particle in the same potential. We are going to analyse sytems in infinite and also in finite volume with periodic boundary conditions.

In infinite volume all the potentials (3.20) tend to zero at infinities implying that the spectrum is continuous and the wave function behaves asymptotically as in a free theory [32, 2]:

$$\psi_{x \to \infty} = \pm \left(e^{-ikx} + S(k)e^{ikx} \right) \quad ; \quad \psi_{x \to -\infty} = e^{-ikx}S(k) + e^{ikx} \tag{4.2}$$

Since the potential is symmetric the wave functions can be chosen to be symmetric or antisymmetric. The appearing scattering phases S(k) can be interpreted both as transmissions through to the potential or alternatively as reflections. These are pure phases and carry information on the interaction. We are going to determine these phases for the rational and hyperbolic models.

In order to describe the periodic versions of the previous potentials we formally place infinitely many particles periodically at distance L: $V_{\rm per}(x) = \sum_{n=-\infty}^{\infty} V(x+nL)$. We demand the wave functions to be periodic as well $\psi(x+L) = \psi(x)$. This means that we analyse the periodic system and not the lattice of particles, which comes with quasi periodic boundary condition and would lead to finite band solutions. Contrary, periodicity implies momentum quantisation and leads to discrete energy spectrum.

A large volume approximation of the spectrum can be obtained from the scattering phase via the Bethe-Yang equation

$$e^{ikL}S(k) = \pm 1$$
 ; $E = k^2$ (4.3)

where the different signs appear for the symmetric and anti-symmetric cases. This picture assumes that we have only one copy of the potential, which is manifested in the scattering phase and periodicity is taken into account for the asymptotic behaviour. Clearly this is only an approximation, which is demonstrated on Figure 1. Typically, there are finite size corrections to this BY equations, which in the relativistic QFT case, can be calculated from the logarithmic derivative of the scattering phase [13].

The finite size spectrum can also be calculated numerically using the truncated Hilbert space method. This is a non-perturbative variational approach, which is based on splitting the Hamiltonian into a soluble and a perturbation part

$$\mathcal{H} = \mathcal{H}_0 + \mathcal{H}_{pert} = -\frac{\partial^2}{\partial x^2} + V_{per}(x),$$
 (4.4)

and using the eigensystem of the free part as the variational basis. Since the spectrum is discrete it can be easily truncated at a given free eigenenergy and the variational method boils down to diagonalizing the truncated Hamiltonian. The free part has even¹ and odd eigenfunctions with the energies

$$\Phi_n^{(+)} = \sqrt{\frac{2}{L}} \cos\left(\frac{2\pi nx}{L}\right) \quad ; \quad \Phi_n^{(-)} = \sqrt{\frac{2}{L}} \sin\frac{2\pi nx}{L} \quad ; \quad \mathcal{H}_0 \Phi_n^{(\pm)} = \left(\frac{2\pi n}{L}\right)^2 \Phi_n^{(\pm)}. \tag{4.5}$$

We then calculate the matrix elements of the perturbation $V_{nm}^{(\pm)} = \langle \Phi_n^{(\pm)} | \hat{\mathcal{H}}_{pert} | \Phi_m^{(\pm)} \rangle$, where due to the symmetry of the potential the even and odd sector is orthogonal to each other. By truncating the Hilbert space with $n \leq N$ we have to diagonalise a finite matrix eventually

$$H_{nm} = \left(\frac{2\pi n}{L}\right)^2 \delta_{nm} + V_{nm} \,. \tag{4.6}$$

If we increase the truncation level N we get a better and better spectrum.

4.1 The rational CMS system

This model describes particles on the whole line, which interact via the potential $V_{\rm rat}$. The Schrödinger equation in the center of mass frame

$$-\frac{\partial^2 \psi(x)}{\partial x^2} + \frac{\lambda(\lambda - 1)}{x^2} \psi(x) = k^2 \psi(x). \tag{4.7}$$

has two solutions out of which

$$\psi(x) = \sqrt{x} J_{\lambda - 1/2}(kx) \tag{4.8}$$

is δ -normalisable [32, 2]. By inspecting the asymptotic behaviour of the Bessel functions, the scattering phase can be extracted

$$S(k) = e^{-i\pi\lambda\operatorname{sgn}(k)} \tag{4.9}$$

The n=0 case should be normalised as $\Phi_0^{(+)}=L^{-1/2}$.

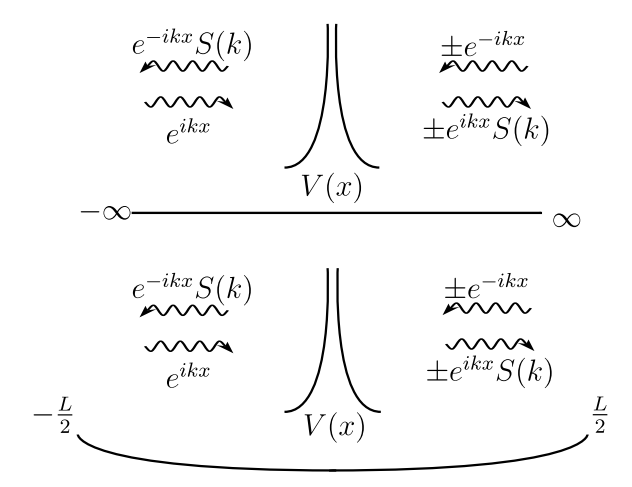


Figure 1: Justification of the Bethe–Yang equations for odd and even wavefunctions. The asymptotic behaviour of the wave function is indicated in infinite volume above. For a large volume system we use the same asymptotic behaviour, and demand the periodicity of the wavefunction.

It is instructive to compare the asymptotic solution with the exact one, which is done on Figure 2. Clearly, the wavefunctions agree only asymptotically. Note also that the physical solution is zero at the origin, which is required by its square integrability around a small region including zero in the potential with $1/x^2$ singularity.

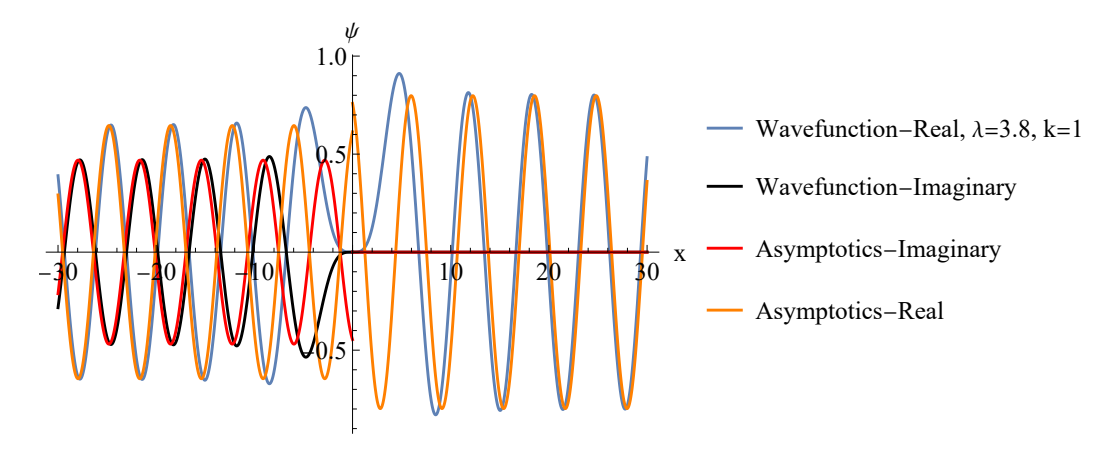


Figure 2: Solution for the rational potential for $\lambda = 3.8$ and k = 1. One can see, that the wavefunction approaches to the asymptotic wavefunctions for large positive and negative values.

4.2 The trigonometric CMS system

Let us now examine the periodic version of the inverse square potential. This interaction potential can be obtained by summing up the contributions of periodically placed particles of disctance L: $\sum_{n=-\infty}^{\infty} \frac{1}{(x+nL)^2} = \left(\frac{\pi}{L}\right)^2 \frac{1}{\sin^2(\frac{\pi x}{L})}$ and leads to the following Schrödinger equation

$$-\frac{\partial^2 \psi(x)}{\partial x^2} + \left(\frac{\pi}{L}\right)^2 \frac{\lambda(\lambda - 1)}{\sin^2(\frac{\pi x}{L})} \psi(x) = k^2 \psi(x). \tag{4.10}$$

This equation also defines the interaction of particles on the circle. In order to find physical solutions we need to specify boundary conditions. If we are interested in the motion of a particle in the periodically placed particles potential we need to demand quasi periodicity, which leads to Bloch waves and band

solutions, similarly to a solid state system. In contrast, here we are interested in the $1/\sin^2$ interaction on the circle thus we demand the periodicity for the wave function. This system allows an analytical solution, which we present now for the symmetric and anti-symmetric sector. In the symmetric case first observe, that the groundstate solution is simply [18]

$$\psi_0^{(+)} = \left| \sin \left(\frac{\pi}{L} x \right) \right|^{\lambda} \quad ; \quad E_0^{(+)} = k_0^2 = \left(\frac{\pi \lambda}{L} \right)^2$$
 (4.11)

We can then look for other symmetric solutions in the form $\psi = \psi_0^{(+)} \tilde{\psi}$ and formulate the eigenvalue problem for $\tilde{E} = E - E_0$ [18]:

$$\mathcal{H}^{(+)}\tilde{\psi} = -\frac{\partial^2 \tilde{\psi}}{\partial x^2} - 2\frac{\pi}{L}\lambda \cot\left(\frac{\pi}{L}x\right) \frac{\partial \tilde{\psi}}{\partial x} = \tilde{E}\tilde{\psi}. \tag{4.12}$$

The reduced Hamiltonian $\mathcal{H}^{(+)}$ acts in an upper triangular way in the symmetric basis:

$$\mathcal{H}^{(+)}\Phi_n^{(+)} = \left(\frac{2\pi}{L}\right)^2 \left(n^2 \Phi_n^{(+)} + n\lambda (\Phi_n^{(+)} + 2\Phi_{n-1}^{(+)} + 2\Phi_{n-2}^{(+)} + \dots + 2\Phi_1^{(+)} + \Phi_0^{(+)})\right), \tag{4.13}$$

The eigenvectors can be calculated iteratively and the eigenvalues of the full Hamiltonian are

$$E_n^{(+)} = E_0^{(+)} + \tilde{E} = k_n^2 = \left(\frac{\pi}{L}\right)^2 (2n+\lambda)^2 \tag{4.14}$$

In the antisymmetric sector we construct the odd groundstate

$$\psi_0^{(-)} = \operatorname{sgn}(x)\cos\left(\frac{\pi x}{L}\right) \left|\sin\left(\frac{\pi x}{L}\right)\right|^{\lambda} \quad ; \quad E_0^{(-)} = \left(\frac{\pi(\lambda+1)}{L}\right)^2 \tag{4.15}$$

and look for the eigenfunctions in the form $\psi = \psi_0^{(-)} \tilde{\psi}$ with $\tilde{E} = E - E_0^{(-)}$. Although $\mathrm{sgn}(x) \cos\left(\frac{\pi x}{L}\right)$ has a finite jump at the origin, the zero of $\left|\sin\left(\frac{\pi x}{L}\right)\right|^{\lambda}$ makes it continues and vanishing there. Similarly to the even case the reduced Hamiltonian

$$\mathcal{H}^{(-)}\tilde{\psi} = -\frac{\partial^2 \tilde{\psi}}{\partial x^2} - 2\frac{\pi}{L} \left(\lambda \cot \left(\frac{\pi}{L} x \right) - \tan \left(\frac{\pi}{L} x \right) \right) \frac{\partial \tilde{\psi}}{\partial x} = \tilde{E}\tilde{\psi}. \tag{4.16}$$

acts an upper triangular way on the even basis, leading to the odd eigenvalues

$$E_n^{(-)} = E_0^{(-)} + \tilde{E} = \left(\frac{\pi}{L}\right)^2 (2n + 1 + \lambda)^2 \tag{4.17}$$

which nicely complement the even ones. The eigenvalues corresponding to odd states can also be obtained in the two-particle formalism in [32, 18].

4.2.1 Finite size corrections and Bethe-Yang equation

We can now compare the exact finite volume wave numbers $k = (\pi/L)(n+\lambda)$ to the one coming from the BY equation

$$e^{ikL}e^{-i\pi\lambda} = \pm 1 \tag{4.18}$$

Clearly the even sector is completely reproduced from the symmetric, while the odd sector from the anti-symmetric BY equations. This is suprising as the wavefunctions are really different. In a QFT the finite size corrections beyond the BY equations are described by the logarithmic derivative of the scattering phase. This quantity is zero here, which indicates that corrections in the non-relativistic theories might have the same origin.

4.2.2 Truncated Hilbert space approach for the trigonometric CMS model

Let us solve eq. (4.10) numerically. In using the truncated Hilbert space method we split the Hamiltonian as

$$\mathcal{H} = \mathcal{H}_0 + \mathcal{H}_{pert} = -\frac{\partial^2}{\partial x^2} + \left(\frac{\pi}{L}\right)^2 \frac{\lambda(\lambda - 1)}{\sin^2(\pi x/L)}$$
(4.19)

The matrix elements in the odd sector are

$$V_{nm}^{(-)} = \left(\frac{\pi}{L}\right)^2 \lambda(\lambda - 1) \frac{2}{L} \int_{-L/2}^{L/2} \frac{\sin\left(\frac{2\pi n}{L}x\right) \sin\left(\frac{2\pi m}{L}x\right)}{\sin^2\left(\frac{\pi}{L}x\right)} = 4\left(\frac{\pi}{L}\right)^2 \lambda(\lambda - 1) \min(n, m). \tag{4.20}$$

In the even sector some matrix elements are divergent, so we regularise them as

$$V_{nm}^{(+)} = 2 \int_{\varepsilon}^{L/2} \Phi_n^{(+)} \mathcal{H}_{pert} \Phi_m^{(+)} dx.$$
 (4.21)

This way only one eigenvalue got corrupted with a very high energy and we could calculate the first N eigenvalues and eigenfunctions. Actually, the singular subspace can be easily identified and one can choose a basis orthogonal to this subspace as

$$\Phi_n = \sqrt{\frac{2}{L}} \sin^2\left(\frac{n\pi x}{L}\right) \,. \tag{4.22}$$

We can calculate the unperturbed energies and the matrix elements of the potential for the new basis:

$$H_{0,nm} = \langle \Phi_n | \mathcal{H}_0 | \Phi_m \rangle = \left(\frac{\pi n}{L}\right)^2 \delta_{nm} \tag{4.23}$$

and

$$V_{nm} = \left(\frac{\pi}{L}\right)^2 \lambda(\lambda - 1) \frac{2}{L} \int_{-L/2}^{L/2} \frac{\sin\left(\frac{\pi n}{L}x\right)^2 \sin\left(\frac{\pi m}{L}x\right)^2}{\sin^2\left(\frac{\pi}{L}x\right)} = \left(\frac{\pi}{L}\right)^2 \lambda(\lambda - 1) \min(n, m). \tag{4.24}$$

As the basis elements are not orthonormal, we need to calculate their inner product matrix and its inverse

$$\Phi_{kl} = \langle \Phi_k | \Phi_l \rangle = \frac{1}{4} \delta_{kl} + \frac{1}{2} \quad ; \quad (\Phi_{kl})^{-1} = 4\delta_{kl} - \frac{8}{2N+1} \,. \tag{4.25}$$

In order to obtain the spectrum we need to diagonalise the following matrix:

$$H_{nm} = (\Phi_{nm})^{-1} \cdot (H_{0,nm} + V_{nm})$$
 (4.26)

After calculating the eigenvalues and eigenstates numerically we obtain a good agreement between the analytical and numerical values. We plotted the first four eigenstates (analytical and numerical) for $\lambda = 2.3$ in figure 3.

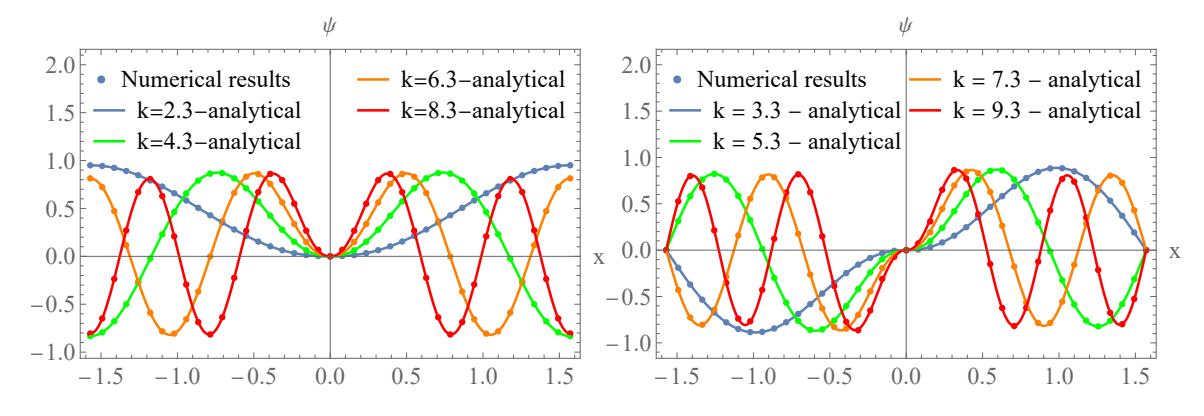


Figure 3: The first four even (on the left) and odd (on the right) eigenstates with their eigenvalues calculated analytically and numerically for $L = \pi$, $\lambda = 2.3$, N = 10.

Next, we should check the convergence of our numerical method. To do this, we keep $\lambda=2.3$ and increase the number of basis elements from N=25. We examined the convergence for the even and odd bases: we calculated the first seven wavenumbers numerically for different number of basis elements and compared to the analytical values. In figures 4 we can see, that the computed wavenumbers nicely converge to the analytically calculated ones.

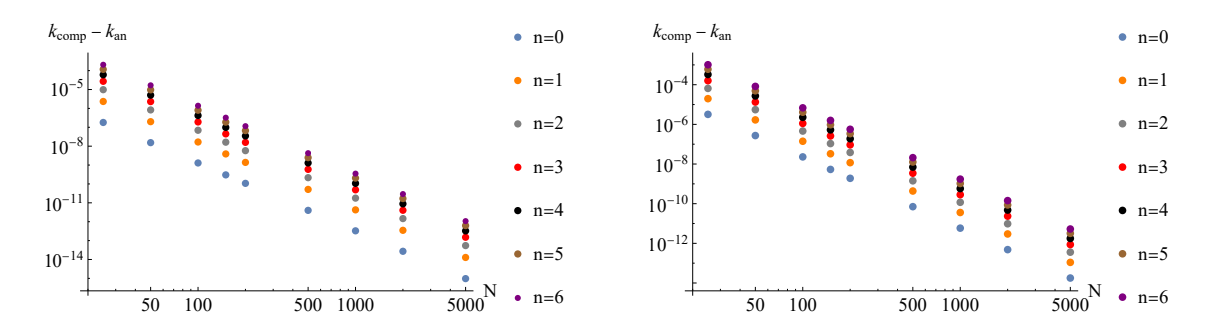


Figure 4: Difference between analytical and numerical results for the first seven even (on the left) and odd (on the right) eigenvalues for different number of basis elements (N) and $\lambda = 2.3$. During our numerical calculations, we calculated the ten lowest eigenvalues using the Arnoldi method, and we compared the first seven eigenvalues to the analytical values.

4.3 The hyperbolic CMS system

The hyperbolic CMS system can be obtained as an analytical continuation of the trigonometric one with the subtitution of $\frac{\pi}{L} \to id$ [19, 32]. We get the following Schrödinger equation:

$$-\frac{\partial^2 \psi(x)}{\partial x^2} + d^2 \frac{\lambda(\lambda - 1)}{\sinh^2(dx)} \psi(x) = E\psi(x). \tag{4.27}$$

Note that the potential is now periodic in the imaginary direction with a period of $\frac{\pi}{d}$. In terms of the momentum $k = \sqrt{E}$ we obtain the following δ -normalisable solution [19]:

$$\psi = {}_{2}F_{1}\left(\frac{1}{2}(\lambda - ik/d), \frac{1}{2}(1 + \lambda - ik/d), \frac{1}{2} + \lambda, y^{2}\right) \frac{1}{\sqrt{y}}(y^{2} - 1)^{-\frac{ik}{2d}}(y^{2})^{\frac{1}{4} + \frac{\lambda}{2}}$$
(4.28)

Here, $y = \tanh dx$ and ${}_2F_1$ is the hypergeometric function. We can multiply the solution in the negative range with a constant phase factor to get even or odd solutions. We now investigate the asymptotics and extract the scattering phase. For $x \to \infty$ we obtain

$$\psi_{x\to\infty} \approx \frac{2^{-1+\lambda}\Gamma(\frac{1}{2}+\lambda)e^{\frac{k\pi}{2d}}}{\sqrt{\pi}\Gamma(\lambda-ik/d)\Gamma(\lambda+ik/d)} \left(\Gamma(\lambda+ik/d)\Gamma(-ik/d)e^{-ikx} + \Gamma(\lambda-ik/d)\Gamma(ik/d)e^{ikx}\right)$$
(4.29)

For $x \to -\infty$, up to a constant phase we got the $x \to -x$ transformed solution, which together give the scattering phase [19, 33]

$$S(k) = \frac{\Gamma(\lambda - ik/d)\Gamma(ik/d)}{\Gamma(\lambda + ik/d)\Gamma(-ik/d)}.$$
(4.30)

The solution and its asymptotics for $\lambda = 2.3$ and k = 2.8 are shown in figure 5.

4.4 The elliptic CMS model

The elliptic CMS model can be thought of as the periodised version of the hyperbolic model

$$\sum_{n=-\infty}^{\infty} \frac{d^2}{\sinh^2(d(x+Ln))} = \wp(x, L, \frac{i\pi}{d}) + \frac{2d\eta_3}{i\pi}$$

$$\tag{4.31}$$

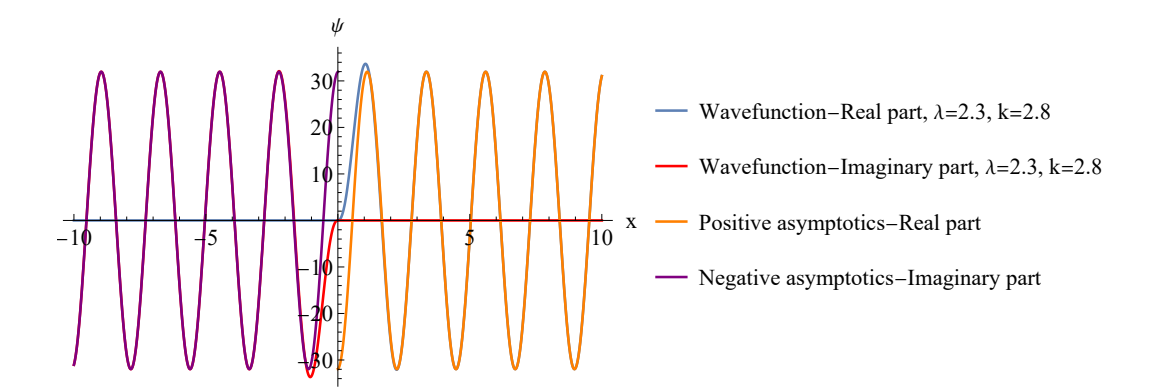


Figure 5: Solutions for the hyperbolic potential for $\lambda = 2.3$ and k = 2.8

The constant η_3 is the imaginary half-period value of the quasi-periodic Weierstrass zeta function, i.e. $\eta_3 = \zeta(\frac{i\pi}{2d})$. For numerical purposes we can also express the potential in terms of the q-polygamma function $\psi_q^{(n)}$, i.e. the n-th derivative of the q-digamma function:

$$\sum_{n=-\infty}^{\infty} \frac{d^2}{\sinh^2(d(x+Ln))} = \frac{-4dL + \psi_{e^{dL}}^{(1)}(\frac{x}{L}) + \psi_{e^{dL}}^{(1)}(\frac{x}{L} - \frac{i\pi}{dL}) + \psi_{e^{dL}}^{(1)}(1 - \frac{x}{L}) + \psi_{e^{dL}}^{(1)}(1 - \frac{x}{L} - \frac{i\pi}{dL})}{L^2}$$
(4.32)

This model was solved for generic coupling by Langmann in [34], perturbatively. For integer λ -s it is a form of the Lamé equation [30] and the solution can be written (for $\lambda = 2$) in a compact form (4.41). However, we present here a non-perturbative approach for general coupling.

We need to solve the following equation:

$$-\frac{\partial^2 \psi(x)}{\partial x^2} + \left(\wp(x, L, \frac{i\pi}{d}) + \frac{2d\eta_3}{i\pi}\right) \lambda(\lambda - 1)\psi(x) = E\psi(x), \qquad (4.33)$$

and we impose periodic boundary condition $\psi(x+L)=\psi(x)$. First, we express the Weierstrass function with the help of the Jacobi elliptic sine function

$$\wp(x) = e_3 + \frac{e_1 - e_3}{\operatorname{sn}^2(\sqrt{e_1 - e_3}x, m)}.$$
(4.34)

where the Weierstrass function values at half periods are $e_1 = \wp(\frac{L}{2})$, $e_2 = \wp(\frac{i\pi}{2d})$ and $e_3 = \wp(\frac{L}{2} + \frac{i\pi}{2d})$ and $\operatorname{sn}(\sqrt{e_1 - e_3}x, m)$ is the elliptic sine function with the module square $m = \frac{e_2 - e_3}{e_1 - e_3}$. After changing variable to $z = \sqrt{e_1 - e_3}x$ we obtain the following equation

$$-\frac{\partial^{2}\psi(z)}{\partial z^{2}} + \frac{\lambda(\lambda - 1)}{\operatorname{sn}^{2}(z, m)}\psi(z) = \left(\frac{E}{e_{1} - e_{3}} - \frac{\lambda(\lambda - 1)e_{3}}{e_{1} - e_{3}} - \frac{\lambda(\lambda - 1)2d\eta_{3}}{i\pi(e_{1} - e_{3})}\right)\psi(z) \equiv h\psi(z). \tag{4.35}$$

where the periodicity requirement takes the form $\psi(z + \sqrt{e_1 - e_3}L) = \psi(z)$. This further can be transformed into a Heun equation. In doing so, we write the wavefunction as

$$\psi(z) = |\operatorname{sn}(z)|^{\lambda} \tilde{\psi}(z). \tag{4.36}$$

where here and from now on we do not write out explicitly the parameter of the Jacobi elliptic function, whenever it leads to no confusion. We then get an equation for $\tilde{\psi}(z)$:

$$-\frac{\partial^2 \tilde{\psi}(z)}{\partial z^2} - 2\lambda \frac{\operatorname{cn}(z) \operatorname{dn}(z)}{\operatorname{sn}(z)} \frac{\partial \tilde{\psi}(z)}{\partial z} + \lambda^2 (m+1) \tilde{\psi}(z) - \lambda (\lambda+1) m \operatorname{sn}^2(z)) \tilde{\psi}(z) = h \tilde{\psi}(z). \tag{4.37}$$

Here we used that $\text{cn}^2 z = 1 - \text{sn}^2 z$ and $\text{dn}^2 z = 1 - m \, \text{sn}^2 z$ [30]. Finally, by substituting $u = \text{sn}^2(z)$ we get the form the Heun equation [35]:

$$\frac{\partial^2 \tilde{\psi}(u)}{\partial u^2} + \left(\frac{\gamma}{u} + \frac{\delta}{u - 1} + \frac{\epsilon}{u - a}\right) \frac{\partial \tilde{\psi}(u)}{\partial u} + \frac{\alpha \beta u - q}{u(u - 1)(u - a)} \tilde{\psi}(u) = 0 \tag{4.38}$$

with the constraint [35]: $\epsilon = \alpha + \beta - \gamma - \delta + 1$, where $a = \frac{1}{m}$, $q = \frac{\lambda^2(1 + \frac{1}{m}) - \frac{h}{m}}{4}$, $\alpha = \frac{\lambda}{2}$, $\beta = \frac{\lambda + 1}{2}$, $\gamma = \frac{1 + 2\lambda}{2}$, $\delta = \frac{1}{2}$ and $\epsilon = \frac{1}{2}$. We can check that the parameters satisfy the constraint relation. The solution of the spectral problem for generic coupling then have the form

$$\psi(z) = |\operatorname{sn}(z)|^{\lambda} H \left(\frac{1}{m}, \frac{\lambda^2 (1 + \frac{1}{m}) - \frac{h}{m}}{4}, \frac{\lambda}{2}, \frac{\lambda + 1}{2}, \frac{1 + 2\lambda}{2}, \frac{1}{2}, \operatorname{sn}^2(z)\right). \tag{4.39}$$

Written in terms of $\operatorname{sn}(z)$ the solution is automatically periodic, but not necessarily regular. Indeed, the quantisation of the momentum comes from requiring regularity. We elaborate on this in the Appendix. For integer λ we also connect the eigenvalues to the eigenvalues of the Lame equation.

$$-\frac{\partial^2 y(\tilde{z})}{\partial \tilde{z}^2} + \lambda(\lambda - 1)m\operatorname{sn}^2(\tilde{z})y(\tilde{z}) = hy(\tilde{z}). \tag{4.40}$$

where $\tilde{z}=z+i\frac{\sqrt{e_1-e_3\pi}}{d}$. We have to distinguish between even and odd λs . The eigenvalues of the even problem are denoted by $b_{\lambda-1}^{2s+2}$, while the corresponding eigenfunctions as $Es_{\lambda-1}^{2s+2}(\tilde{z})$ [36], while in the odd λ case the eigenvalues are denoted as $a_{\lambda-1}^{2s+1}$ and correspond to the Lamé functions $Ec_{\lambda-1}^{2s+1}(\tilde{z})$ [36]. Here s labels the solutions.

For integer λ s the Lame solutions can also be written in terms of Weierstrass σ - and ζ -functions. For comparison we present here the simplest solution for (4.33), which appears for $\lambda = 2$ [37, 38, 39].

$$\psi(x) = \frac{\sigma(x+z)}{\sigma(x)} e^{-\zeta(z)x} \tag{4.41}$$

and has energy $E=-\wp(z)+\frac{4d\eta_3}{i\pi}$. We can ensure periodicity $\psi(x)=\psi(x+L)$ by looking for z in the form $z=i\alpha_n$, and demanding

$$\eta_1 \alpha_n + i\zeta(i\alpha_n)\omega_1 = \pi n \tag{4.42}$$

which has a solution for any n. The physical solution is $\psi(x) + \psi(-x)$, which we compared against the Lame and Heun solutions for this particular λ . The corresponding energy is $E_n = -\wp(i\alpha_n) + \frac{4d\eta_3}{i\pi}$.

4.5 Numerical examination of the elliptic Calogero-Moser system

Let us move to the numerical analysis of the system. We use the method we highlighted at the beginning of the section. Although the method works for any λ , we present the results for integer λ s, where comparison with the Lame solution is also available. For $\lambda=4$, $L=\pi$ and d=1 we calculated the first four even and odd eigenstates and compared them to eq. (4.39) and eq. (A.14) for even and odd eigenstates in figure 6.

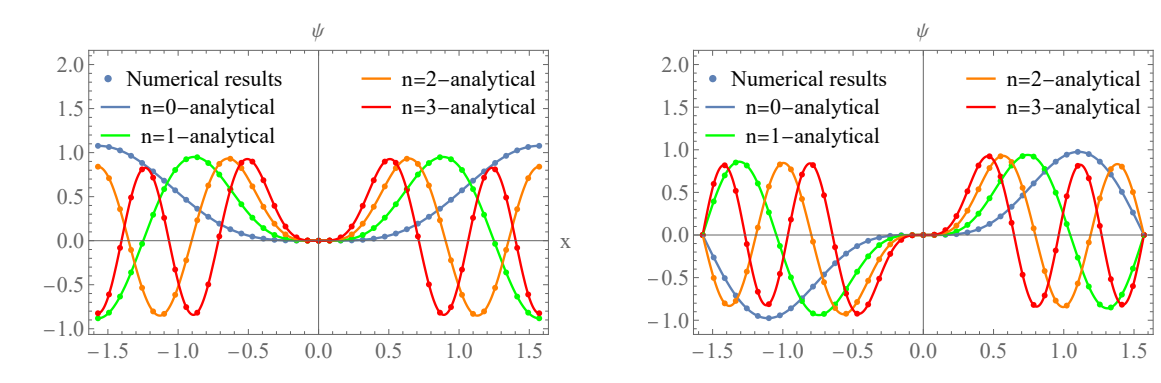


Figure 6: The first four even eigenstates with their eigenvalues calculated analytically and numerically and normalised for $L = \pi$, d = 1, $\lambda = 4$, N = 10.

We also tested the convergence of our numerical solutions by calculating the first seven eigenvalues for different number of basis elements, and we could see that the difference between the momenta, calculated from Lamé eigenvalues, and the momenta, calculated numerically, decreases systematically when increasing the number of basis elements.

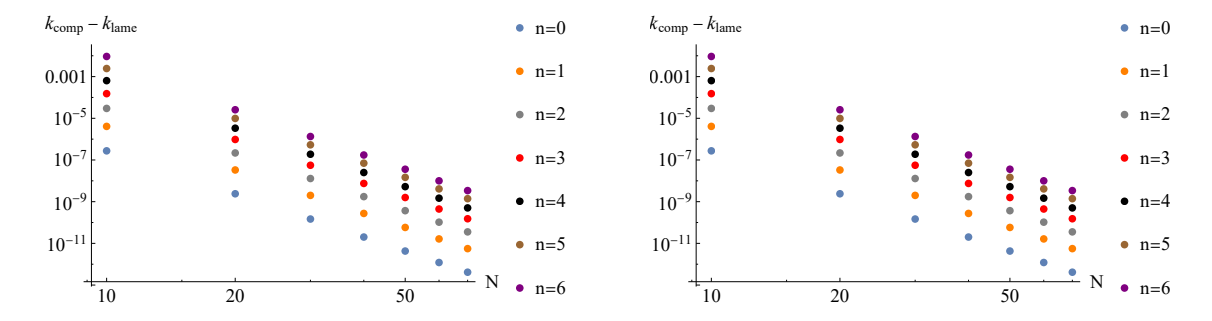


Figure 7: Difference between analytical and numerical results for the first seven even ($\lambda = 3$, on the left) and odd ($\lambda = 4$, on the right) momenta for different number of basis elements (N) for the hyperbolic potential.

4.6 Comparison between the Bethe–Yang equation and the wavenumbers of the elliptic potential

Let us examine now the validity of the Bethe–Yang equation for this potential. Recall, that the scattering coefficient is given by eq. (4.30). However, now the Bethe–Yang equation does not hold exactly neither in its symmetric nor its antisymmetric form. To see this, we calculated the difference between the wavenumbers computed numerically and the wavenumbers given with the help of Lamé coefficients for different coupling constants and lengths. In figure 8 we can see, that the difference between the BY wavenumbers and the exact ground state momentum decreases for small and large lengths and small coupling constants. It would be very interesting to describe this difference in terms of the scattering phase.

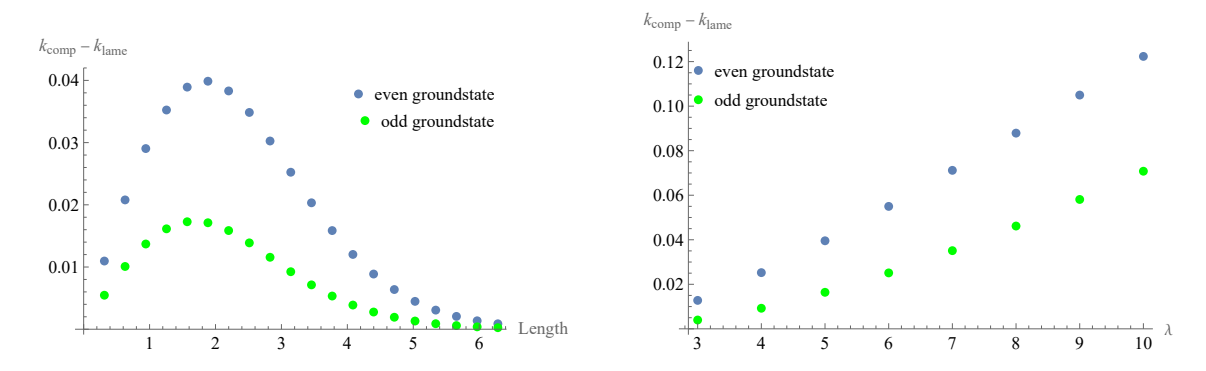


Figure 8: Validity of the Bethe–Yang equations for the even and odd ground states at various lengths (left) and coupling constants (right). The BY equations describes the system more accurately at large and small volumes and small coupling constants.

5 Ruijsenaars–Schneider models and the truncated Hilbert space method

Having analysed the non-relativistic limits we turn back to the investigations of the RS models. We focus on the two particle case in the center of mass frame, where the Schrödinger equation takes the form

$$H_{\text{red}}\psi(q) = (f_{+}(q)T^{+}f_{+}(-q) + f_{+}(-q)T^{-}f_{+}(q))\psi(q) = 2\cosh(\theta)\psi(q).$$
 (5.1)

where $T^{+}f(q) = f(q+i)$ and $T^{-}f(q) = f(q-i)$.

We first present the infinite-volume RS models, which are the rational and hyperbolic systems. As the potential vanishes at the infinities we have free scattering solutions (3.11):

$$\psi_{q \to -\infty}(q) = e^{i\theta q} + S(\theta)e^{-i\theta q} \quad ; \quad \psi_{q \to \infty}(q) = \pm (e^{-i\theta q} + S(\theta)e^{i\theta q}) \tag{5.2}$$

Note that here q is not the coordinate, rather the conjugate variable to the rapidity. We present first the phase for the hyperbolic model and obtain the rational case as its limit.

We then turn to the periodic versions of these potentials. Recall that here the periodicity is in q, not in the physical coordinate. The real coordinate of the particle is $x = \frac{q}{\cosh \theta}$, implying that the effective spatial periodicity depends on the particle's momentum. Consequently, the notion of a periodic volume loses its simple geometric meaning in x, and manifests itself only in q-space. This feature is closely related to the relativistic invariance of the model, which is preserved even though the system is defined in a finite volume.

An approximate spectrum can be obtained by the Bethe-Yang equation

$$e^{i\theta L}S(\theta) = \pm 1 \tag{5.3}$$

which quantises the rapidities and leads to energies via $E = 2 \cosh \theta$.

The exact finite volume solution is available for the trigonometric case, which we present explicitly. We compare the result to the Bethe–Yang equation and see that it is exact. As the relevant analytical solution of the elliptic model for general coupling is not known we adapt the truncated Hilbert space method to difference equations and benchmark the result against the explicitly known integer λ and trigonometric cases. Finally, we use this method to obtain the spectrum of the generic elliptic model.

In adapting the truncated Hilbert space method we split our Hamiltonian into the already introduced free part and a perturbation

$$H_{\rm red} = H_{\rm free} + H_{\rm pert} \,. \tag{5.4}$$

where the perturbed Hamiltonian is given by

$$H_{\text{pert}} = (f_{+}(q)f_{+}(-q-i) - 1)T^{+} + (f_{+}(-q)f_{+}(q-i) - 1)T^{-}.$$
(5.5)

The basis introduced in the non-relativistic setting in the variable q is an eigenbasis of the free Hamiltonian

$$H_{\text{free}}\Phi_n^{(\pm)} = (T^+ + T^-)\Phi_n^{(\pm)} = 2\cosh\left(\frac{2\pi}{L}n\right)\Phi_n^{(\pm)}$$
 (5.6)

We then calculate the matrix elements of the perturbing Hamiltonian. Since it is parity invariant we can work separately in the even and odd subspaces:

$$H_{\text{pert},kl}^{(\pm)} = \langle \Phi_k^{(\pm)} | H_{\text{pert}} | \Phi_l^{(\pm)} \rangle \tag{5.7}$$

We now truncate our Hilbert space by keeping elements below the cutoff $n \leq N$ and diagonalize the truncated reduced Hamiltonian H_{red} . By increasing N we get a better approximation.

5.1 The hyperbolic RS model

The hyperbolic model was examined in details in [29]. For two particles in the center of mass frame the Schrödinger equation takes the form (5.1) with the "potential"

$$f_{+}^{\text{hyp}}(q) = \sqrt{\frac{\sinh(d(q+i\lambda))}{\sinh(dq)}}.$$
 (5.8)

As the potential vanishes at the infinities we should have free scattering solutions (3.11) and the aim is to determine the scattering phase, which we denote by $S^{\text{hyp}}(\theta)$. This job was done by Ruijsenaars observing that the Schrödinger equation has also a dual analogue [29], see also [40, 41]. This implied a difference equation directly for $S^{\text{hyp}}(\theta)$ in θ [7], which was analogous to the unitarity and crossing requirement of the soliton-soliton scattering phase and had the minimal solution

$$S^{\text{hyp}}(\theta) = -\exp\left(2i\int_0^\infty \frac{dy}{y} \frac{\sinh(d(1-\lambda)y)\sinh(\pi y - d\lambda y)}{\sinh(dy)\sinh(\pi y)}\sin(y\theta)\right). \tag{5.9}$$

This solution can be directly related to the sine-Gordon expression by setting

$$d = \frac{\pi p}{2} \quad ; \quad \lambda = \frac{1}{p} \tag{5.10}$$

In these calculations we set the speed of light to c=1 from the beginning. If instead we restore its form and analyse its $c\to\infty$ limit we can recover the scattering phase (4.30) of the hyperbolic CMS model.

5.2 The rational RS model

The rational RS model is the $d \to 0$ limit of the hyperbolic model and is defined by the Schrödinger equation (5.1), where the rational function f_+^{rat} is the double-degenerate limit of the elliptic function:

$$f_{+}^{\rm rat} = \sqrt{\frac{q + i\lambda}{q}} \,. \tag{5.11}$$

The scattering phase of the rational model can be obtained in the limit $d \to 0$ of the hyperbolic one (5.9) $S^{\text{rat}}(z) = \lim_{d\to 0} S^{\text{hyp}}(z)$, which takes a particularly simple form:

$$S^{\text{rat}}(\theta) = -\lim_{d \to 0} \exp\left(2i \int_0^\infty \frac{dy}{y} \frac{\sinh\left((1-\lambda)y\right) \sinh(\pi y/d - \lambda y)}{\sinh y \sinh(\pi y/d)} \sin(y\theta/d)\right) =$$

$$= -\exp\left(2i(1-\lambda) \int_0^\infty \frac{dy}{y} \sin(y\theta)\right) = \exp\left(-i\pi\lambda \operatorname{sgn}(\theta)\right),$$
(5.12)

Clearly, the rational scattering coefficient does not depend on the magnitude of the rapidity only on its sign. It is actually the same as its non-relativistic limit, which is the rational CMS model.

5.3 The trigonometric RS model

The trigonometric RS model is the periodic version of the rational model and is defined in the two-particle sector in the center of mass frame by the Schrödinger equation (5.1) with the potential function

$$f_{+}^{\text{trig}}(q) = \left(\frac{\sin\left(\pi(q+i\gamma)/L\right)}{\sin(\pi q/L)}\right)^{1/2},\tag{5.13}$$

This model yields back the rational RS model for $L \to \infty$. This is the relativistic version of the trigonometric CMS model, and can be solved analytically in a similar method. We are going to present the analytical solutions first, and then we implement the truncated Hilbert space method for difference equations and compare the results.

5.3.1 Analytical solution of the trigonometric RS model

Let us look for even solutions. First observe [42, 33] that the ground state function

$$\psi_0(q) = \sqrt{\prod_{k=0}^{\infty} \frac{e^{i\frac{2\pi}{L}q} - e^{-\frac{2\pi}{L}k}}{e^{i\frac{2\pi}{L}q} - e^{-\frac{2\pi}{L}(k+\lambda)}} \frac{e^{-i\frac{2\pi}{L}q} - e^{-\frac{2\pi}{L}k}}{e^{-i\frac{2\pi}{L}q} - e^{-\frac{2\pi}{L}(k+\lambda)}}}$$
(5.14)

solves our system and gives the ground state energy

$$E_0 = 2\cosh\left(\frac{\pi}{L}\lambda\right). \tag{5.15}$$

To get excited states we use a similar method to the trigonometric Calogero--Moser system: again, we look for solutions in the form $\psi = \psi_0 \tilde{\psi}$. After substituting and dividing by the vacuum state we get the reduced equation

$$H_{\text{red}}\tilde{\psi}(q) = \frac{\sin\left(\frac{\pi}{L}(q+i\lambda)\right)}{\sin\left(\frac{\pi}{L}q\right)}\tilde{\psi}(q+i) + \frac{\sin\left(\frac{\pi}{L}(q-i\lambda)\right)}{\sin\left(\frac{\pi}{L}q\right)}\tilde{\psi}(q-i) = E\tilde{\psi}(q). \tag{5.16}$$

The Hamiltonian $H_{\rm red}$ acts on the even basis spanned by $\Phi_n^{(+)}$ as:

$$H_{\text{red}}\Phi_n^{(+)} = 2\cosh\left(\frac{\pi}{L}(2n+\lambda)\right)\left(\Phi_n^{(+)} + \Phi_{n-1}^{(+)} + \dots + \frac{1}{2}\Phi_0^{(+)}\right) - \\ -2\cosh\left(\frac{\pi}{L}(2n-\lambda)\right)\left(\Phi_{n-1}^{(+)} + \dots + \frac{1}{2}\Phi_0^{(+)}\right).$$
(5.17)

implying that $\{\Phi_0^{(+)},\Phi_1^{(+)},\dots,\Phi_n^{(+)}\}$ is an invariant subspace and its elements form an upper triangular matrix. The eigenvalues of the Hamiltonian are the diagonal elements

$$E_n = 2\cosh(\theta_n) , \quad \theta_n = \frac{\pi}{L}(2n+\lambda) .$$
 (5.18)

and the eigenvectors can be calculated iteratively.

The odd ground state wavefunction can be written in terms of the even one as

$$\psi_0^{\text{odd}} = \psi_0(q) \cos\left(\frac{\pi}{L}q\right) \operatorname{sgn}(q)$$
 (5.19)

where the continuity follows from $\psi_0(0) = 0$. The corresponding eigenvalue is

$$E_0^{\text{odd}} = 2\cosh\left(\frac{\pi}{L}(1+\lambda)\right). \tag{5.20}$$

We can seek for solutions in the product form $\psi^{\text{odd}} = \psi_0^{\text{odd}} \tilde{\psi}_{\text{odd}}$. After dividing the Schrödinger equation by the odd vacuum state we get

$$\frac{\sin\left(\frac{\pi}{L}(q+i\lambda)\right)}{\sin\left(\frac{\pi}{L}q\right)}\cos\left(\frac{\pi}{L}(q+i)\right)\tilde{\psi}_{\text{odd}}(q+i) +
+ \frac{\sin\left(\frac{\pi}{L}(q-i\lambda)\right)}{\sin\left(\frac{\pi}{L}q\right)}\cos\left(\frac{\pi}{L}(q-i)\right)\tilde{\psi}_{\text{odd}}(q-i) = E^{\text{odd}}\tilde{\psi}_{\text{odd}}(q)\cos\left(\frac{\pi}{L}q\right).$$
(5.21)

Using the even basis (4.5) we obtain

$$H_{\text{red}}\Phi_{n}^{(+)} = 2\cosh\left(\frac{\pi}{L}\left((2n+1)+\lambda\right)\right)\Phi_{n}^{(+)} + \left(2\cosh\left(\frac{\pi}{L}\left((2n+1)+\lambda\right)\right) - 2\cosh\left(\frac{\pi}{L}\left((2n-1)-\lambda\right)\right)\right)\left(\Phi_{n-2}^{(+)} + \Phi_{n-4}^{(+)} + \dots\right) + \left(2\cosh\left(\frac{\pi}{L}\left((2n-1)+\lambda\right)\right) - 2\cosh\left(\frac{\pi}{L}\left((2n+1)-\lambda\right)\right)\right)\left(\Phi_{n-1}^{(+)} + \Phi_{n-3}^{(+)} + \dots\right),$$
(5.22)

so the action of H_{red} on $\{\Phi_0^{(+)}, \dots, \Phi_n^{(+)}\}$ yields an upper triangular matrix with the following eigenvalues:

$$E_n^{\text{odd}} = 2\cosh\left(\theta_n\right), \quad \theta_n = \frac{\pi}{L}\left(2n+1+\lambda\right),$$
 (5.23)

which complete our even-state rapidities. Clearly we get back both the odd and even momenta of the trigonometric CM model. The difference, however is, that in the RS case the rapidities agree with wavenumbers and not the momenta. This is related to the fact that the wave function has the form $e^{i\theta q}$ and not e^{ipx} .

5.3.2 Comparison to BY equations

Similarly to the trigonometric CM model, substituting the quantised rapidities (5.18) (for even states) and (5.23) (for odd states) into eq. (5.3) we can see, that the BY equations hold for both the even and odd cases, the latter giving the antisymmetric BY equations. Again, as in case of the trigonometric Calogero–Moser system, we can conclude that the Bethe–Yang equations hold for any length L.

5.4 Numerical calculations for the trigonometric RS model

We proceed to solve the trigonometric RS model numerically. We follow the generic procedure of splitting the Hamiltonian into a free and interacting part and calculate the matrix elements of the perturbation directly. We start with the odd matrix elements

$$H_{\text{pert},kl}^{(-)} = \langle \Phi_k^{(-)} | H_{\text{pert}} | \Phi_l^{(-)} \rangle =$$

$$= \frac{2}{L} \int_{-L/2}^{L/2} dq \sin\left(\frac{2\pi kq}{L}\right) \left(f_+^{\text{trig}}(q) f_+^{\text{trig}}(-q-i) - 1\right) \sin\left(\frac{2\pi l(q+i)}{L}\right) +$$

$$+ \frac{2}{L} \int_{-L/2}^{L/2} dq \sin\left(\frac{2\pi kq}{L}\right) \left(f_+^{\text{trig}}(-q) f_+^{\text{trig}}(q-i) - 1\right) \sin\left(\frac{2\pi l(q-i)}{L}\right).$$
(5.24)

The matrix elements of the full Hamiltonian can be calculated as

$$H_{\text{red},kl}^{(-)} = H_{\text{free},kl}^{(-)} + H_{\text{pert},kl}^{(-)},$$
 (5.25)

which, after truncation, can be diagonalized numerically. This provides approximate eigenvalues and eigenvectors. By increasing the truncation levels the method nicely converges.

Although the similar procedure works for even states the singular behaviour of the potential at the origin $|q|^{-\frac{1}{2}}$ prevents the method from converging well. So instead we introduced a new basis:

$$\Phi_k = \sqrt{\frac{2}{L}} \sqrt{\sin^2(\pi q/L)} \cos\left(\frac{2\pi}{L} kq\right) . \tag{5.26}$$

As this basis is not orthonormal we have to proceed as we did in the case of the CMS models. First, we calculate the matrix elements of the free Hamiltonian in this basis:

$$H_{\text{free},kl}^{\text{even}} = \langle \Phi_k | H_{\text{free}} | \Phi_l \rangle = \cosh\left(\frac{\pi}{L}\right) \cosh\left(\frac{2\pi}{L}k\right) \delta_{kl} - \frac{1}{2} \cosh\left(\frac{\pi}{L}(2k-1)\right) \delta_{k,l+1} - \frac{1}{2} \cosh\left(\frac{\pi}{L}(2k+1)\right) \delta_{k,l-1} + \cosh\left(\frac{\pi}{L}\right) \delta_{k0} \delta_{l0} - \frac{1}{2} \cosh\left(\frac{\pi}{L}\right) (\delta_{k0} \delta_{l1} + \delta_{l0} \delta_{k1}).$$

$$(5.27)$$

The matrix elements of the perturbed Hamiltonian must be calculated numerically. It has the following matrix elements:

$$H_{\text{pert},kl}^{\text{even}} = \langle \Phi_k | H_{\text{pert}} | \Phi_l \rangle =$$

$$= \int_{-L/2}^{L/2} dq \; \Phi_k(q) \left(f_+^{\text{trig}}(q) f_+^{\text{trig}}(-q-i) - 1 \right) \Phi_k(q+i) +$$

$$\int_{-L/2}^{L/2} dq \; \Phi_k(q) \left(f_+^{\text{trig}}(-q) f_+^{\text{trig}}(q-i) - 1 \right) \Phi_k(q-i) .$$
(5.28)

Again, we use for f_+ the function given by eq. (5.13). In this case, the basis elements are not orthonormal, so we need to calculate the inverse of the matrix obtained from the inner products. The inner product in this basis can be given as

$$\langle \Phi_k | \Phi_l \rangle = \frac{1}{2} \delta_{kl} - \frac{1}{4} (\delta_{k,l-1} + \delta_{k,l+1}) + \frac{1}{2} \delta_{k0} \delta_{l0} - \frac{1}{4} (\delta_{k0} \delta_{l1} + \delta_{l0} \delta_{k1}). \tag{5.29}$$

To determine the eigenvalues and eigenvectors, we need to calculate the inverse of the inner product. If we act on the truncated basis $\{\Phi_0, \Phi_1, \dots, \Phi_N\}$ we get the following inverse inner product:

$$(\Phi_{kl})^{-1} = \begin{pmatrix} N+1 & 2N & 2N-2 & 2N-4 & \dots & 2\\ 2N & 4N & 4N-4 & 4N-8 & \dots & 4\\ 2N-2 & 4N-4 & 4N-4 & 4N-8 & \dots & 4\\ 2N-4 & 4N-8 & 4N-8 & 4N-8 & \dots & 4\\ \vdots & \vdots & \vdots & \vdots & \ddots & \vdots\\ 2 & 4 & 4 & 4 & \dots & 4 \end{pmatrix} .$$
 (5.30)

The matrix elements of the full Hamiltonian can be calculated as

$$H_{\text{red},kl}^{\text{even}} = \left(\Phi_{kj}\right)^{-1} \left(H_{\text{free},jl}^{\text{even}} + H_{\text{pert},jl}^{\text{even}}\right). \tag{5.31}$$

We have to calculate the eigenvalues and eigenvectors of $(H_{\text{red}}^{\text{even}})_{kl}$ to get the even eigenstates and their energies and wavenumbers numerically. After getting the odd and even eigenvalues E_k we can calculate the corresponding quantised rapidities as

$$\theta_n = \arccos(E_k/2). \tag{5.32}$$

We plotted the first four odd and even eigenfunctions for $L=2\pi$ and N=10 in figure 9. The numerical states and eigenvalues correspond nicely to the analytical states and their eigenvalues, which satisfy the Bethe–Yang equations.

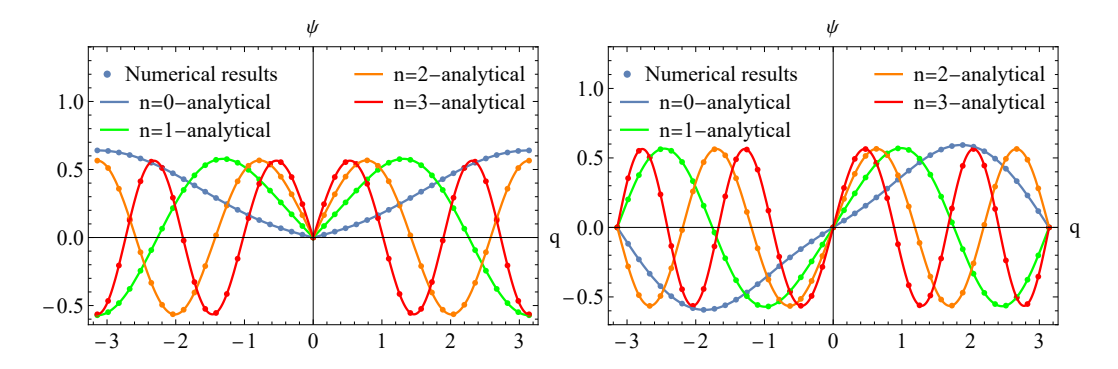


Figure 9: The first four even (left) and odd (right) eigenstates with their eigenvalues calculated analytically and numerically and normalised for $L = 2\pi$, $\lambda = 2.3$, N = 10.

5.5 The elliptic RS model

Finally, let us turn our attention to the elliptic RS model, which is the finite-volume version of the hyperbolic RS model. We want to solve the Schrödinger equation (5.1) with the elliptic potential f_+^{ell} written in terms of the Weierstrass sigma functions [27]:

$$f_{+}^{\text{ell}}(q) = \sqrt{\frac{\sigma(q+i\lambda, L, i\pi/d)}{\sigma(q, L, i\pi/d)}}.$$
(5.33)

Although the sigma functions are quasi-periodic with the relation

$$\sigma(q+L) = -e^{2\eta_1(q+L/2)}\sigma(q), \qquad (5.34)$$

where η_1 is the Weierstrass zeta-function at L/2, the Hamiltonian $H_{\text{red}}^{\text{ell}}$ itself is periodic. To see this, we can write it in the explicit form:

$$H_{\text{red}}^{\text{ell}} = g_{+}(q)T^{+} + g_{-}(q)T^{-},$$
 (5.35)

where

$$g_{\pm}(q) = \sqrt{\frac{\sigma(q \pm i\lambda, L, i\pi/d)}{\sigma(q, L, i\pi/d)}} \sqrt{\frac{\sigma(q \mp i\lambda \pm i, L, i\pi/d)}{\sigma(q \pm i, L, i\pi/d)}}$$
(5.36)

and observe the periodicity $g_{\pm}(q+L) = g_{\pm}(q)$.

It is useful to see how the hyperbolic theory is recoverd in the limit $L \to \infty$. Since the sigma function behaves as [27]:

$$\sigma(q, \infty, id) = \frac{\sinh dq}{d} \exp\left(-\frac{d^2}{6}q^2\right). \tag{5.37}$$

we can obtain the limiting cases

$$g_{\pm}(q) \xrightarrow{L \to \infty} \exp\left(\frac{d^2}{6}\lambda(\lambda - 1)\right) \sqrt{\frac{\sinh(d(q \pm i\lambda))}{\sinh(dq)}} \sqrt{\frac{\sinh(d(q \mp i\lambda \pm i))}{\sinh(d(q + i))}}$$
 (5.38)

which leads to the following relations of the Hamiltonians

$$H_{\text{red}}^{\text{ell}} \xrightarrow{L \to \infty} \exp\left(\frac{d^2}{6}\lambda(\lambda - 1)\right) \left(f_+^{\text{hyp}}(q)T^+ f_+^{\text{hyp}}(-q) + f_+^{\text{hyp}}(-q)T^- f_+^{\text{hyp}}(q)\right), \tag{5.39}$$

They thus agree up to a multiplicative factor

$$H_{\text{red}}^{\text{ell}} \xrightarrow{L \to \infty} CH_{\text{red}}^{\text{hyp}}, \quad C = \exp\left(\frac{d^2}{6}\lambda(\lambda - 1)\right)$$
 (5.40)

This means that the finite volume version of the hyperbolic model is actually $C^{-1}H_{\text{red}}^{\text{ell}}$. In order to take care of this difference and support the correct comparison with the Bethe–Yang equations we parametrize the energy eigenvalues in the elliptic Schrödinger equation in the following form:

$$\left(f_{+}^{\text{ell}}(q)T^{+}f_{+}^{\text{ell}}(-q) + f_{+}^{\text{ell}}(-q)T^{-}f_{+}^{\text{ell}}(q)\right)\psi(q) = 2C\cosh(\theta)\psi(q). \tag{5.41}$$

The perturbative solution was constructed in [43] at generic coupling. Here we determine the eigenvalues and eigenvectors numerically using the non-perturbative truncated Hilbert space method. We benchmark the solution against the explicitly known solution for $\lambda = 2$, which we recall now from [44].

5.5.1 Analytical solution for $\lambda = 2$

Similarly to the elliptic Calogero-Moser system the elliptic RS model can be solved using transcendental functions [44]. We present, again the simplest solution for the elliptic RS model for $\lambda = 2$. First, we consider the following functions which solve our elliptic difference equation:

$$\mathcal{F}(q,y) = \frac{\sigma(q+z)}{\sigma(q+i)\sigma(q-i)} \exp(2\pi i q/L + iqy)$$
(5.42)

with the following energy eigenvalue:

$$E = \frac{1}{\sigma(q)} \left(\sigma(q+i) \exp(2\pi/L + y) \frac{\sigma(q-i+z)}{\sigma(q+z)} + \sigma(q-i) \exp(-2\pi/L - y) \frac{\sigma(q+i+z)}{\sigma(q+z)} \right). \tag{5.43}$$

This energy depends on q for generic y and z values. However, it is an elliptic function with the periods L and π/d , so it is constant if the residue of one of its two simple poles vanish [44, 30]. The pole at q = 0 vanishes if

$$y = -\frac{2\pi}{L} - \frac{1}{2} \ln \frac{\sigma(z-i)}{\sigma(z+i)}. \tag{5.44}$$

In addition of the condition for the constant energy, we need \mathcal{F} to be periodic in L. If we seek for the coefficient z in the form of $z = i\alpha_n$ we get the following condition:

$$4\eta_1 \alpha_n - L \ln \frac{\sigma(i\alpha_n - i)}{\sigma(i\alpha_n + i)} = 2(n+2)\pi.$$
 (5.45)

Substituting back the values of $z = i\alpha_n$ into (5.43) we get back the energies calculated for even states for even n values starting with n = 0 and the energies of odd states for odd values starting with n = 1. The following eigenfunctions coincide with the numerical odd and even eigenfunctions, respectively [44]:

$$\begin{cases} \psi_n = \mathcal{F}(q, \alpha_n) - \mathcal{F}(-q, \alpha_n) & n \text{ odd} \\ \psi_n = \operatorname{sgn}(q)(\mathcal{F}(-q, \alpha_n) - \mathcal{F}(q, \alpha_n)) & n \text{ even} \end{cases}$$
 (5.46)

The analytical and numerical wavefunctions are shown in figure 10 for the first four odd and even states for $\lambda = 2$ and $L = \pi$.

5.5.2 Numerical solution of the elliptic RS model

We proceed with the numerical solution for generic coupling as in the case of the trigonometric RS model. We start with the odd subspace spanned by $\Phi_n^{(-)}$ and calculate the matrix elements of the perturbing Hamiltonian numerically

$$H_{\text{pert},kl}^{(-)} = \langle \Phi_k^{(-)} | H_{\text{pert}} | \Phi_l^{(-)} \rangle = \int_{-L/2}^{L/2} dq \, \Phi_k^{(-)}(q) \left(f_+^{\text{ell}}(q) f_+^{\text{ell}}(-q-i) - 1 \right) \Phi_l^{(-)}(q+i) + \int_{-L/2}^{L/2} dx \, \Phi_k^{(-)}(q) \left(f_+^{\text{ell}}(-q) f_+^{\text{ell}}(q-i) - 1 \right) \Phi_k^{(-)}(q-i)$$

$$(5.47)$$

In the even case we could use the even basis $\Phi_n^{(+)}$, however, the convergence problem due to the $|q|^{-1/2}$ behaviour persists, so we switched to the basis Φ_n . After calculating the perturbed matrices,

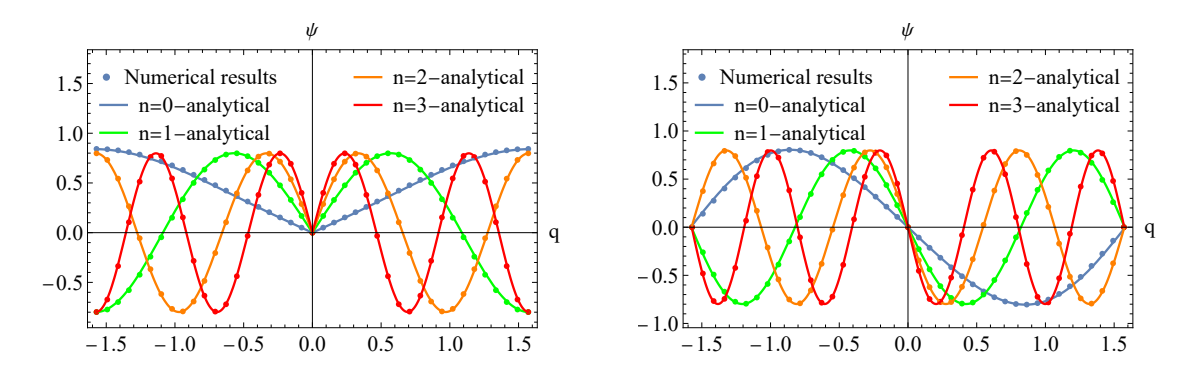


Figure 10: The first four even (left) and odd (right) eigenstates of the elliptic RS model with their eigenvalues calculated analytically and numerically and normalised for $L = \pi$, $\lambda = 2$, N = 10.

we calculate again the eigenvalues and eigenvectors of the truncated Hamiltonians (5.25) and (5.31). From any eigenvalue we can calculate the corresponding rapidity θ_n .

We plotted the first four even and odd eigenstates for $L=2\pi$ and $d=5\pi/16$ in figure 11. These parameters correspond to p=5/8 in the sine-Gordon model.

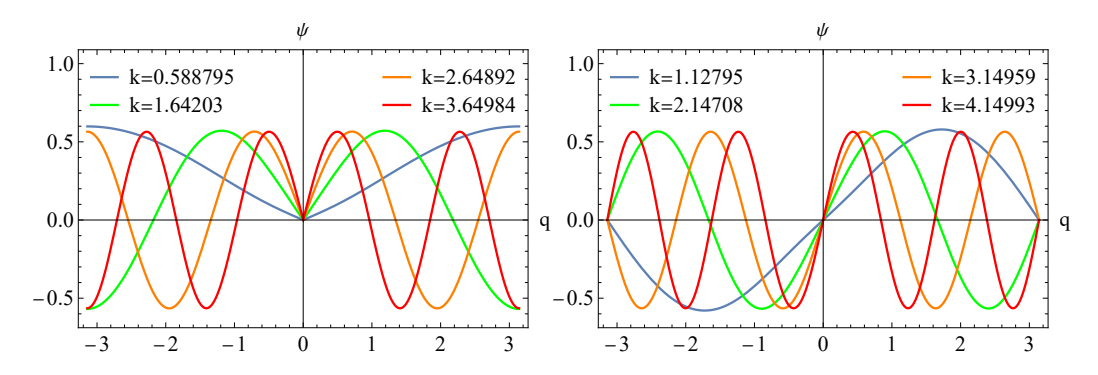


Figure 11: Numerically calculated even (left) and odd (right) states for the elliptic RS model. We used the parameters $L=2\pi$, $d=5\pi/16$, $\lambda=8/5$ and N=10.

5.5.3 Comparison to Bethe-Yang equations

As in the case of the elliptic CMS model, the BY equations does not hold exactly for the calculated rapidities. To see this, we calculated the difference between the numerically computed quantised rapidities and their BY analogues for the even and odd ground states for different lengths and coupling constants λ . We can see in figure 12, that the difference between the rapidities is smaller for larger lengths and smaller couplings, which is also true for the elliptic CMS models.

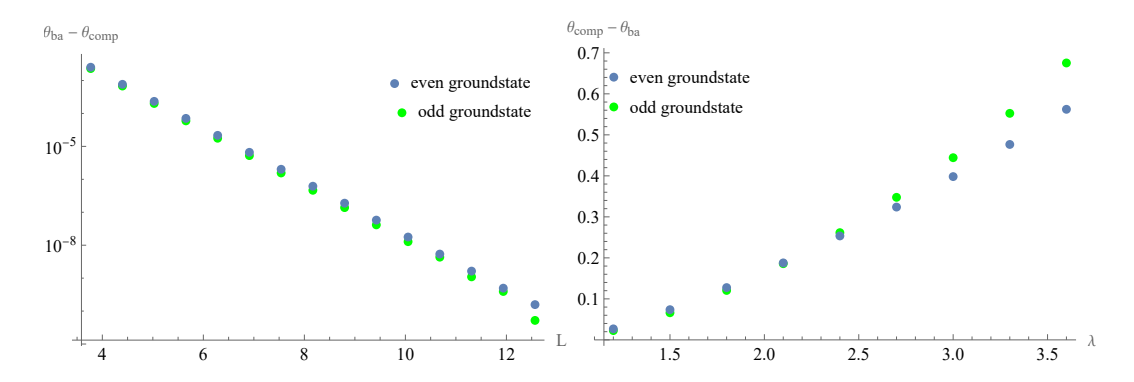


Figure 12: Validity of the BY equations for the even and odd ground states at various lengths (left) and coupling constants (right). The Bethe–Yang equation describes the system more accurately at large volumes and small coupling constants.

6 Comparing the quantum elliptic RS model to the finite volume quantum sG theory

Let us point out an important difference between quantum field theories and quantum many body systems. The vacuum in a quantum field theory is a complicated state, which is populated by particle—antiparticle pairs, while in quantum mechanics it is empty. When a QFT is obtained as a thermodynamic limit of a many body system, the vacuum is typically a strongly interacting state. The finite volume sine-Gordon theory, for instance, can be obtained as the continuum scaling limit of the staggered XXZ spin chain [21]. The finite volume sine-Gordon vacuum corresponds to the anti-ferromagnetic XXZ vacuum, with infinitely many interacting real Bethe roots. As a consequence, the ground state energy has a non-trivial volume dependence. In the following we compare the energy difference between a two soliton state and the vacuum to the spectrum of the elliptic RS model. We normalise the elliptic spectrum, such that at large volumes it reproduces the hyperbolic model (5.40).

6.1 Free case

First, let us examine the free theories. This corresponds to p = 1 in the sine-Gordon theory, when the scattering phase vanishes. The quantization condition for two moving free fermions is

$$ML\sinh\theta = 2\pi n + \pi \tag{6.1}$$

where n is an integer. Taking M=1, the corresponding energy difference to the vacuum is

$$E = 2\cosh\theta. \tag{6.2}$$

The free RS model is given by $d = \frac{\pi}{2}$ and $\lambda = 1$. The Bethe ansatz is exact and quantises the rapidities as

$$\theta L = 2\pi n + \pi \tag{6.3}$$

while the energy is given by

$$E_{\rm RS} = 2\cosh\theta. \tag{6.4}$$

This means, that the spectrum of the two free theories coincide only at very large lengths, where we can take the approximation $\sinh\theta\approx\theta$. This is related to the fact that the wave function in the sine-Gordon case is e^{ipx} , while in the RS case it is $e^{i\theta q}$. This former expression is required by the correct dispersion relation.

6.2 Interacting case

Next, we compare the spectrum of the elliptic RS model and the sG model. We do the comparison only numerically. We should keep in mind, that after calculating the eigenvalues of the RS model with

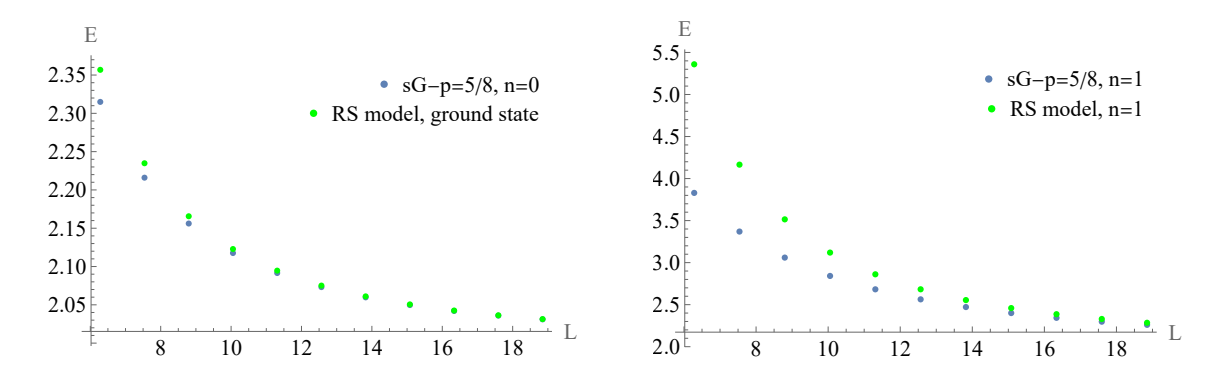


Figure 13: Ground state and first even excited state energies for the RS and first and second corrected two-soliton energies for the sG models for different system volumes. We used p = 5/8.

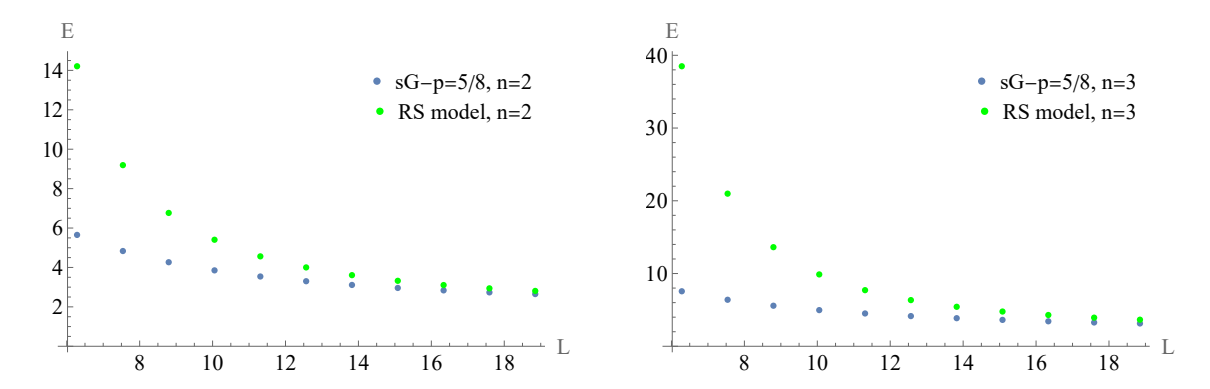


Figure 14: Second and third even excited state energies for the RS and third and fourth corrected two-soliton energies for the sG models for different system volumes. We used p = 5/8.

the truncated Hilbert space method, we should multiply them with the inverse of the multiplicative factor given in (5.40)

$$C^{-1} = \exp\left(-\frac{d^2}{6}\lambda(\lambda - 1)\right) = \exp\left(-\frac{\pi^2}{24}(1 - p)\right)$$
 (6.5)

to get the correct spectrum.

At larger volumes we expect that both the sine-Gordon theory and the RS model approximate the Bethe–Yang quantisation lines. However, the two BY equations are different, which has its roots in the different coordinate representations, similarly to the free case. Indeed, the BY equations in the sine-Gordon theory are (2.15)

$$e^{iL\sinh\theta}S(\theta) = 1$$

In contrast, in the RS model they read as

$$e^{iL\theta}S(\theta) = 1$$

while the corresponding energies have the same form $E = 2 \cosh \theta$. Thus already at the BY level we recognize differences, which is due to the different forms of the asymptotic wave functions. This difference could have disappeared in the exact spectrum, but we can do this comparison only numerically.

In figures 13 and 14 we compare the spectra of the elliptic RS and the finite-volume sG model at p=5/8 for different lengths. In case of the sine-Gordon model, we subtracted the vacuum energy E_0 from the soliton energies. As expected, the two spectra approach each other for large lengths, where they approximate the Bethe ansatz equations, and the difference between the energies is smaller for smaller values of n.

We can clearly see on the figures that the two models' energies differ. So the difference appears not only because they approach different BY energies at large energies, but they are really different at finite sizes. We investigated the cutoff (N) depends of these results and observed that errors were smaller than the dots on the figures and decreased with increasing the cutoff.

Conclusions

In this paper we compared the finite-size spectrum of the sine-Gordon quantum field theory with the spectrum of the elliptic Ruijsenaars–Schneider model. The original motivation was to test whether the well-established equivalence between the infinite-volume sine-Gordon theory and the hyperbolic RS model extends to finite volume. Although the two models share the same scattering matrix in infinite volume, finite-size effects in relativistic QFTs are governed by the scattering phases not only via the Bethe–Yang equations but also by vacuum polarization (Lüscher) corrections. No analogous, generally accepted finite-volume framework exists for quantum many-body systems, so we pursued a predominantly numerical comparison.

Since there are no non-perturbative exact results for the elliptic RS model, we adapted the non-perturbative truncated Hilbert-space method to difference operators and benchmarked it in several cases (integer coupling, the trigonometric limit), where analytical results are available. Our numerical study—restricted to the two-particle sector in the center-of-mass frame—shows that the two spectra differ at finite volume. The differences can be traced to (i) the nontrivial vacuum structure of the field theory (vacuum polarisation by particle—antiparticle pairs) versus the trivial vacuum of the quantum many-body system, and (ii) the distinct form of the free wavefunctions: in the QFT they are plane waves in coordinate space, whereas in the RS models plane waves live in the coordinate dual to rapidity.

In the large-volume limit both theories are governed at leading order by the Bethe–Yang equations, but we find that subleading (finite-size) corrections behave differently: the Bethe–Yang quantization is exact in the rational/trigonometric correspondences, while in the hyperbolic/elliptic case it is only asymptotic. This suggests that finite-size corrections for many-body systems may nevertheless be expressible in terms of scattering data (for example, via derivatives of the S-matrix), but that the precise mechanism differs from the Lüscher/TBA machinery of relativistic QFTs.

A natural next step is to develop an analytic description of these finite-size corrections for quantum many-body systems (elliptic RS and their non-relativistic limits). Clarifying whether and how such corrections can be written solely in terms of the S-matrix would both deepen the RS-sine-Gordon correspondence and broaden our understanding of finite-volume effects in integrable quantum mechanics.

Promising next steps include deriving Lüscher-like formulae for many-body systems and searching for a TBA-style formulation that captures the elliptic finite-volume corrections.

Acknowledgements

We are indebted to Rob Klabbers for the many useful discussions and comments on the manuscript. We also thank János Balog and László Fehér for reading the manuscript and the useful suggestions. ZB thanks the Marc Kac center in Kraków for hospitality during the final stages of this work. ZB was supported in part by a Priority Research Area DigiWorld grant under the Strategic Programme Excellence Initiative at the Jagiellonian University (Kraków, Poland). The research was also supported by the grant K134946 of NKFIH.

A Details of the elliptic CMS model

In this Appendix we detail the calculations of the elliptic CMS model. We map the differential equation to the Heun equation and investigate its regularity properties. We then compare for integer λ s the results to the Lame solution.

A.1 Analytical solution

We need to solve the following equation:

$$-\frac{\partial^2 \psi(x)}{\partial x^2} + \left(\wp(x, L, \frac{i\pi}{d}) + \frac{2d\eta_3}{i\pi}\right) \lambda(\lambda - 1)\psi(x) = E\psi(x), \tag{A.1}$$

As we already shown, using functional identities with Jacobi elliptic functions and changing the variable to $z = \sqrt{e_1 - e_3}x$ we obtain the differential equation

$$-\frac{\partial^2 \psi(z)}{\partial z^2} + \frac{\lambda(\lambda - 1)}{\operatorname{sn}^2(z, m)} \psi(z) = \left(\frac{E}{e_1 - e_3} - \frac{\lambda(\lambda - 1)e_3}{e_1 - e_3} - \frac{\lambda(\lambda - 1)2d\eta_3}{i\pi(e_1 - e_3)}\right) \psi(z) \equiv h\psi(z). \tag{A.2}$$

where the periodicity requirement is $\psi(z+\sqrt{e_1-e_3}L)=\psi(z)$. This is not of the standard Lame form, but using the identity $\operatorname{sn}(z,m)^{-2}=m\operatorname{sn}(z+i\frac{\sqrt{e_1-e_3}\pi}{d},m)^2$ we can write

$$-\frac{\partial^2 \psi(z)}{\partial z^2} + m\lambda(\lambda - 1)\operatorname{sn}^2\left(z + i\frac{\sqrt{e_1 - e_3}\pi}{d}, m\right)\psi(z) = h\psi(z) \tag{A.3}$$

We can introduce the shifted variable $\tilde{z}=z+i\frac{\sqrt{e_1-e_3\pi}}{d}$ but the periodicity requirement needs to be imposed at an imaginary shifted postion $\tilde{z}-i\frac{\sqrt{e_1-e_3\pi}}{d}$. This is very non-standard so we transform instead the equation (A.2) into a Heun equation.

Let us start with the even solutions and write the wavefunction as

$$\psi(z) = |\operatorname{sn}(z)|^{\lambda} \tilde{\psi}(z). \tag{A.4}$$

and substitute $u = \operatorname{sn}^2(z)$ to get the form the Heun equation [35]:

$$\frac{\partial^2 \tilde{\psi}(u)}{\partial u^2} + \left(\frac{\gamma}{u} + \frac{\delta}{u-1} + \frac{\epsilon}{u-a}\right) \frac{\partial \tilde{\psi}(u)}{\partial u} + \frac{\alpha \beta u - q}{u(u-1)(u-a)} \tilde{\psi}(u) = 0 \tag{A.5}$$

with the parameters $a=\frac{1}{m},\ q=\frac{\lambda^2(1+\frac{1}{m})-\frac{h}{m}}{4},\ \alpha=\frac{\lambda}{2},\ \beta=\frac{\lambda+1}{2},\ \gamma=\frac{1+2\lambda}{2},\ \delta=\frac{1}{2}$ and $\epsilon=\frac{1}{2}$. The solution of the spectral problem then have the form

$$\psi(z) = |\operatorname{sn}(z)|^{\lambda} H \left(\frac{1}{m}, \frac{\lambda^2 (1 + \frac{1}{m}) - \frac{h}{m}}{4}, \frac{\lambda}{2}, \frac{\lambda + 1}{2}, \frac{1 + 2\lambda}{2}, \frac{1}{2}, \operatorname{sn}^2(z)\right). \tag{A.6}$$

We now investigate the regularity of the solution. Recall that the general Heun equation has four singular points at 0, 1, a and ∞ . The general Heun function $Hl(a, q, \alpha, \beta, \gamma, \delta, u)$ is constructed to be regular at u=0, however, the singularities at 1, a and ∞ persist in these solutions [35]. As in our case $a=\frac{1}{m}\geq 1$ and $-1\leq \operatorname{sn}^2(z)\leq 1$ the singularities at a and ∞ should cause no concerns, however, the solution remains singular around 1, which corresponds to $\operatorname{sn}^2(\frac{\sqrt{e_1-e_3}L}{2})$, the point in the middle of the periodicity strip. To understand to regularity requirement we investigate the convergence properties of the power series expansion around u=0. It is known [35], that the radius of convergence of these solutions is usually 1, and the solutions are singular at 1, however the radius of convergence can be extended to $\frac{1}{m}$ for certain values of h. Let us see, how the requirement comes out.

First, we construct the generic solutions as a powever series [35]:

$$Hl(z) = \sum_{r=0}^{\infty} c_r z^r \,. \tag{A.7}$$

Plugging black into the differential we obtain the following recursion [35]:

$$\begin{cases}
P_r c_{r-1} + S_r c_r + R_r c_{r+1} = 0 & r \ge 1 \\
-q c_0 + a \gamma c_1 = 0,
\end{cases}$$
(A.8)

with

$$P_r = (r - 1 + \alpha)(r - 1 + \beta)$$

$$S_r = -q - r((r - 1 + \gamma)(1 + a) + a\delta + \epsilon)$$

$$R_r = (r + 1)(r + \gamma)a$$
(A.9)

where in our case

$$\begin{cases}
m(\lambda + 2r - 2)(\lambda + 2r - 1)c_{r-1} + (h - (\lambda + 2r)^2(m+1))c_r + \\
+ (2r + 2)(2\lambda + 2r + 1)c_{r+1} = 0 \\
(h - \lambda^2(1+m))c_0 + 2(2\lambda + 1)c_1 = 0.
\end{cases}$$
(A.10)

We need to determine the convergence of a general power series (A.7) given by a three-term recursion (A.8). This can be done by using the simplest form of Poincaré-Perron theory [35]. In a three-term

recursion, if, after dividing by suitable function of r, $P_r \to P$, $S_r \to S$ and $R_r \to R$ as $r \to \infty$, we can define the following characteristic equation:

$$P + S\rho + R\rho^2 = 0. \tag{A.11}$$

The Poincaré-Perron theory states [35] that if the characteristic equation has two roots ρ_1 and ρ_2 with different moduli and if $|\rho_1| < |\rho_2|$ then generically the series (A.7) has a radius of convergence of $|\rho_2|^{-1}$. However, if S_r can be written as $S_r = h - Q_r$, where h does not depend on r, then for certain values of h the series (A.7) converges up to $|\rho_1|^{-1}$. These values of h can be given by a continued fraction equation [35]:

$$h - Q_0 = \frac{R_0 P_1}{h - Q_1 - \frac{R_1 P_2}{h - Q_2 - \dots}}.$$
(A.12)

In our case, the characteristic equation (A.11), $m-(m+1)\rho+\rho^2=0$, has the roots $\rho_1=1$ and $\rho_2=m$. So, unless h is given by the continued fraction (A.12), the series (A.7) has a convergence radius of 1. However, it can be extended to $\frac{1}{m}$ if h satisfies (A.12), which is the quantisation of momenta.

Let us now extend the analysis for the odd solutions for our equation (A.2), which is searched for in the form of

$$\psi = \operatorname{sgn}(z)\operatorname{cn}(z,m)|\operatorname{sn}(z,m)|^{\lambda}\tilde{\psi}. \tag{A.13}$$

After performing the same computations as in the even case, we get the following solution:

$$\tilde{\psi}(z) = Hl\left(\frac{1}{m}, \frac{\lambda^2 + \frac{(\lambda+1)^2}{m} - \frac{h}{m}}{4}, \frac{\lambda+1}{2}, \frac{\lambda+2}{2}, \frac{1+2\lambda}{2}, \frac{3}{2}, \operatorname{sn}^2(z)\right)$$
(A.14)

If we consider again the solutions as infinite power series we get the following recursion:

$$\begin{cases}
m(\lambda + 2r - 1)(\lambda + 2r)c_{r-1} + (h - (\lambda + 2r + 1)^2 - m(\lambda + 2r)^2)c_r + \\
+ (2r + 2)(2\lambda + 2r + 1)c_{r+1} = 0 \\
(h - (\lambda + 1)^2 - m\lambda^2))c_0 + 2(2\lambda + 1)c_1 = 0.
\end{cases}$$
(A.15)

The quantization of the momentum comes from the same continued fraction equation (A.12).

A.2 Correspondence between the eigenvalues of the elliptic potential and the eigenvalues of the Lamé equation

Interestingly, the admitted values h for integer λ correspond to certain eigenvalues of the Lamé equation. To see this, let us write the Lamé equation's Jacobian form [36]:

$$-\frac{\partial^2 y(\tilde{z})}{\partial \tilde{z}^2} + \lambda(\lambda - 1)m\operatorname{sn}^2(\tilde{z})y(\tilde{z}) = hy(\tilde{z}). \tag{A.16}$$

Note that the literature uses the notation $n = \lambda - 1$.

Let us start with the even solutions (A.6). In order to see the correspondence we use a power series expansion of the form [36]:

$$y(\tilde{z}) = \operatorname{cn}\tilde{z} \operatorname{dn}\tilde{z} \sum_{r=0}^{\infty} c_r \operatorname{sn}^{2r+1}\tilde{z}.$$
(A.17)

and also demand convergence up to $\operatorname{sn}(\tilde{z}) \sim 1$. Plugging back the solution into the differential equation we get the following recursion [36]:

$$m(2r - \lambda + 2)(\lambda + 2r + 1)c_{r-1} + (h - (2r + 2)^{2}(m+1))c_{r} + (2r + 2)(2r + 3)c_{r+1} = 0.$$
 (A.18)

For even values of λ we can substitute $2r = \lambda - 2 + 2r'$ to get

$$2r'm(2\lambda + 2r' - 1)c_{r-1} + (h - (\lambda + 2r')^2(m+1))c_r + (\lambda + 2r')(\lambda + 2r' + 1)c_{r+1} = 0.$$
 (A.19)

which gives the same continued fraction as eq. (A.10). Having the same continued fraction expansion they lead to the same requirements for the values h as in the Heun case. Note that these eigenfunctions

are denoted as $b_{\lambda-1}^{2s+2}$, while the eigenvalues of the odd Lamé functions as $Es_{\lambda-1}^{2s+2}(z)$ [36]. Here s labels the solutions.

We can get the correspondence for odd λ values by looking for Lamé functions in the form of [36]

$$y(\tilde{z}) = \operatorname{cn}\tilde{z} \operatorname{dn}\tilde{z} \sum_{r=0}^{\infty} c_r \operatorname{sn}^{2r} \tilde{z}.$$
(A.20)

The recursion is given by

$$m(2r - \lambda + 1)(\lambda + 2r)c_{r-1} + (h - (2r+1)^2(m+1))c_r + (2r+1)(2r+2)c_{r+1} = 0.$$
(A.21)

which by setting $2r = \lambda - 1 + 2r'$ can be transformed to

$$2r'm(2\lambda + 2r' - 1)c_{r-1} + (h - (\lambda + 2r')^2(m+1))c_r + (\lambda + 2r')(\lambda + 2r' + 1)c_{r+1} = 0,$$
 (A.22)

which is the same recursion as eq. (A.19). These eigenvalues are denoted as $a_{\lambda-1}^{2s+1}$ and correspond to the even Lamé functions $Ec_{\lambda-1}^{2s+1}(z)$ [36].

Now, we should turn our attention to the odd solutions (A.14). We can show the correspondence with the Lamé eigenvalues for integer λ values again. First, to show for even λ 's we write the solution of the Lamé functions in form of [36]

$$y(\tilde{z}) = \operatorname{cn}\tilde{z} \sum_{r=0}^{\infty} c_r \operatorname{sn}^{2r} \tilde{z}.$$
(A.23)

We get the following recursion [36]:

$$m(2r-\lambda)(\lambda+2r+1)c_{r-1} + (h-(2r+1)^2 - 4r^2m)c_r + (2r+1)(2r+2)c_{r+1} = 0.$$
(A.24)

Setting $2r = \lambda + 2r'$ we get

$$2r'm(2\lambda + 2r' - 1)c_{r-1} + (h - (\lambda + 2r' + 1)^2 - (\lambda + 2r')^2m)c_r + (\lambda + 2r' + 1)(\lambda + 2r' + 2)c_{r+1} = 0.$$
(A.25)

which confirms the correspondence again. This time, the involved Lamé eigenvalues are $a_{\lambda-1}^{2s+1}$ and correspond to the even Lamé functions $Ec_{\lambda-1}^{2s+1}(z)$ [36].

To show for odd λ 's we need the following type of Lamé solution [36]:

$$y(z) = \operatorname{cn} z \sum_{r=0}^{\infty} c_r \operatorname{sn}^{2r+1} z$$
. (A.26)

The recursion following from this form is [36]

$$m(2r - \lambda + 1)(\lambda + 2r)c_{r-1} + (h - (2r + 2)^2 - (2r + 1)^2 m)c_r + (2r + 2)(2r + 3)c_{r+1} = 0.$$
 (A.27)

Again, let us substitute $2r = \lambda - 1 + 2r'$:

$$2r'm(2\lambda + 2r' - 1)c_{r-1} + (h - (\lambda + 2r' + 1)^2 - (\lambda + 2r')^2m)c_r + (\lambda + 2r' + 1)(\lambda + 2r' + 2)c_{r+1} = 0,$$
(A.28)

which is exactly the same recursion as eq. (A.25). The corresponding eigenvalues are $b_{\lambda-1}^{2s+2}$ corresponding to the odd Lamé functions $Es_{\lambda-1}^{2s+2}(z)$ [36].

References

- [1] P. Dorey, Exact S matrices, in: Eotvos Summer School in Physics: Conformal Field Theories and Integrable Models, 1996, pp. 85–125. arXiv:hep-th/9810026.
- [2] L. Samaj, Z. Bajnok, Introduction to the statistical physics of integrable many-body systems, Cambridge University Press, Cambridge, 2013.

- [3] G. Mussardo, Statistical Field Theory: An Introduction to Exactly Solved Models in Statistical Physics, Oxford University Press, 2010. doi:10.1093/acprof:oso/9780199547586.001.0001.
- [4] A. Zamolodchikov, A. Zamolodchikov, Factorized s-matrices in two dimensions as the exact solutions of certain relativistic quantum field theory models, Annals of Physics 120 (1979) 253–291. doi:10.1016/0003-4916(79)90391-9.
- [5] R. Rajaraman, Solitons and Instantons: An Introduction to Solitons and Instantons in Quantum Field Theory, North-Holland, 1982.
- [6] S. N. M. Ruijsenaars, H. Schneider, A New Class of Integrable Systems and Its Relation to Solitons, Annals Phys. 170 (1986) 370–405. doi:10.1016/0003-4916(86)90097-7.
- [7] S. N. M. Ruijsenaars, First order analytic difference equations and integrable quantum systems,
 J. Math. Phys. 38 (2) (1997) 1069. doi:10.1063/1.531809.
- [8] M. Hallnäs, S. Ruijsenaars, Joint eigenfunctions for the relativistic Calogero-Moser Hamiltonians of hyperbolic type. II. The two- and three-variable cases (1 2017). arXiv:1607.06672.
- [9] N. Belousov, S. Derkachov, S. Kharchev, S. Khoroshkin, Baxter operators in Ruijsenaars hyperbolic system II: bispectral wave functions, Annales Henri Poincare 25 (7) (2024) 3259–3296.
 arXiv:2303.06382, doi:10.1007/s00023-023-01385-z.
- [10] M. Hallnäs, Calogero-Moser-Sutherland systems, 2023. arXiv:2312.12932.
- [11] M. Hallnäs, E. Langmann, Elliptic Integrable Systems and Special Functions, 2024. arXiv: 2408.05821.
- [12] C. Yang, C. Yang, Thermodynamics of a one-dimensional system of bosons with repulsive delta-function interaction, Journal of Mathematical Physics 10 (7) (1969) 1115–1122. doi:10.1063/1.1664947.
- [13] A. Zamolodchikov, Thermodynamic bethe ansatz in relativistic models: Scaling three state potts and lee-yang models, Nuclear Physics B 342 (1990) 695–720. doi:10.1016/0550-3213(90) 90333-9.
- [14] M. Luscher, Volume dependence of the energy spectrum in massive quantum field theories. i. stable particle states, Communications in Mathematical Physics 104 (1986) 177–206. doi:10.1007/BF01211589.
- [15] M. Luscher, Volume dependence of the energy spectrum in massive quantum field theories. ii. scattering states, Communications in Mathematical Physics 105 (1986) 153–188. doi:10.1007/BF01211097.
- [16] Z. Bajnok, R. A. Janik, Four-loop perturbative Konishi from strings and finite size effects for multiparticle states, Nucl. Phys. B 807 (2009) 625-650. arXiv:0807.0399, doi:10.1016/j. nuclphysb.2008.08.020.
- [17] F. Calogero, Solution of the one-dimensional N body problems with quadratic and/or inversely quadratic pair potentials, J. Math. Phys. 12 (1971) 419–436. doi:10.1063/1.1665604.
- [18] B. Sutherland, Exact results for a quantum many-body problem in one dimension. II, Physical Review A 5 (3) (1972) 1372.
- [19] B. Sutherland, Beautiful models: 70 years of exactly solved quantum many-body problems, World Scientific Publishing Company, 2004.
- [20] J. Moser, Three integrable hamiltonian systems connected with isospectral deformations, in: Surveys in applied mathematics, Elsevier, 1976, pp. 235–258.
- [21] C. Destri, H. J. De Vega, Unified approach to thermodynamic Bethe Ansatz and finite size corrections for lattice models and field theories, Nucl. Phys. B 438 (1995) 413–454. arXiv: hep-th/9407117, doi:10.1016/0550-3213(94)00547-R.

- [22] C. Destri, H. J. de Vega, Nonlinear integral equation and excited states scaling functions in the sine-Gordon model, Nucl. Phys. B 504 (1997) 621-664. arXiv:hep-th/9701107, doi:10.1016/ S0550-3213(97)00468-9.
- [23] G. Feverati, F. Ravanini, G. Takacs, Nonlinear integral equation and finite volume spectrum of Sine-Gordon theory, Nucl. Phys. B 540 (1999) 543-586. arXiv:hep-th/9805117, doi:10.1016/ S0550-3213(98)00747-0.
- [24] T. R. Klassen, E. Melzer, On the relation between scattering amplitudes and finite size mass corrections in QFT, Nucl. Phys. B 362 (1991) 329–388. doi:10.1016/0550-3213(91)90566-G.
- [25] M. P. Heller, R. A. Janik, T. Lukowski, A New derivation of Luscher F-term and fluctuations around the giant magnon, JHEP 06 (2008) 036. arXiv:0801.4463, doi:10.1088/1126-6708/ 2008/06/036.
- [26] D. Bombardelli, A next-to-leading Luescher formula, JHEP 01 (2014) 037. arXiv:1309.4083, doi:10.1007/JHEP01(2014)037.
- [27] S. N. M. Ruijsenaars, Complete Integrability of Relativistic Calogero-moser Systems and Elliptic Function Identities, Commun. Math. Phys. 110 (1987) 191. doi:10.1007/BF01207363.
- [28] J. Balog, Relativistic trajectory variables in 1+1 dimensional Ruijsenaars-Schneider type models (2 2014). arXiv:1402.6990.
- [29] S. N. M. Ruijsenaars, Sine-gordon solitons vs. relativistic calogero-moser particles, in: Integrable Structures of Exactly Solvable Two-Dimensional Models of Quantum Field Theory, Springer, 2001, pp. 273–292.
- [30] E. T. Whittaker, G. N. Watson, A course of modern analysis, Courier Dover Publications, 2020.
- [31] S. N. M. Ruijsenaars, Ruijsenaars-Schneider model, Scholarpedia 4 (5) (2009) 7760, revision #124978. doi:10.4249/scholarpedia.7760.
- [32] L. Samaj, Introduction to integrable many-body systems I, Acta physica slovaca 58 (2008) 811–946.
- [33] G. Arutyunov, Elements of Classical and Quantum Integrable Systems, Springer, 2019.
- [34] E. Langmann, Explicit solution of the (quantum) elliptic calogero–sutherland model, in: Annales Henri Poincare, Vol. 15, Springer, 2014, pp. 755–791.
- [35] A. Ronveaux, F. M. Arscott, Heun's differential equations, Clarendon Press, 1995.
- [36] E. Ince, V. The Periodic Lame Functions, Proceedings of the Royal Society of Edinburgh 60 (1) (1940) 47–63.
- [37] E. T. Whittaker, G. N. Watson, A Course of Modern Analysis, 4th Edition, Cambridge University Press, Cambridge, London and New York, 1927.
- [38] S. N. M. Ruijsenaars, Generalized lame functions. i. the elliptic case, Journal of Mathematical Physics 40 (3) (1999) 1595–1626. doi:10.1063/1.532822.
- [39] R. Klabbers, J. Lamers, How Coordinate Bethe Ansatz Works for Inozemtsev Model, Commun. Math. Phys. 390 (2) (2022) 827–905. arXiv:2009.14513, doi:10.1007/s00220-021-04281-x.
- [40] S. N. M. Ruijsenaars, Finite-dimensional soliton systems, Integrable and superintegrable systems (1990) 165–206.
- [41] S. N. M. Ruijsenaars, Systems of Calogero-Moser Type, Springer New York, New York, NY, 1999, pp. 251–352. doi:10.1007/978-1-4612-1410-6_7.
- [42] J. Van Diejen, et al., On the diagonalization of difference calogero-sutherland systems, in: Symmetries and Integrability of Difference Equations. CRM Proceedings and Lecture Notes, Vol. 9, 1996, pp. 79–89.

- [43] E. Langmann, M. Noumi, J. Shiraishi, Construction of eigenfunctions for the elliptic ruijsenaars difference operators, Communications in Mathematical Physics 391 (3) (2022) 901–950.
- [44] S. N. M. Ruijsenaars, On Relativistic Lame Functions, Springer New York, New York, NY, 2000, pp. 421–440. doi:10.1007/978-1-4612-1206-5_26.